



CHORUS

This is the accepted manuscript made available via CHORUS. The article has been published as:

Testing the threshold expansion for three-particle energies at fourth order in $\phi^{\{4\}}$ theory

Stephen R. Sharpe

Phys. Rev. D **96**, 054515 — Published 26 September 2017

DOI: [10.1103/PhysRevD.96.054515](https://doi.org/10.1103/PhysRevD.96.054515)

Testing the threshold expansion for three-particle energies at fourth order in ϕ^4 theory

Stephen R. Sharpe^{1,*}

¹*Physics Department, University of Washington, Seattle, WA 98195-1560, USA*

(Dated: September 7, 2017)

A relativistic formalism for relating the energies of the states of three scalar particles in finite volume to infinite volume scattering amplitudes has recently been developed. This formalism has been used to predict the energy of the state closest to threshold in an expansion in powers of $1/L$, with L the box length. This expansion has been tested previously by a perturbative calculation of the threshold energy in $\lambda\phi^4$ theory, working to third order in λ and up to $\mathcal{O}(1/L^6)$ in the volume expansion. However, several aspects of the predicted threshold behavior do not enter until fourth (three-loop) order in perturbation theory. Here I extend the perturbative calculation to fourth order and find agreement with the general prediction. This check also requires a two-loop calculation of the infinite-volume off-shell two-particle scattering amplitude near threshold. As a spin-off, I check the threshold expansion for two particles to the same order, finding agreement with the result that follows from Lüscher's formalism.

Keywords: finite volume, relativistic scattering theory, lattice QCD

* e-mail: srsharpe@uw.edu

I. INTRODUCTION

There is considerable interest in developing theoretical formalism to allow lattice QCD to determine the properties of resonances for which some of the decay channels involve three or more particles. Such formalism is needed for the study of most of the strong-interaction resonances that appear in nature, e.g. the ω meson and the Roper baryon. Specifically, what is needed on the theoretical side is a quantization condition that relates the energies of multiparticle states in a finite volume to the infinite-volume scattering amplitudes of these particles. While such a quantization has long been known for two particles (based on Refs. [1, 2] and subsequent generalizations), the three particle quantization condition is relatively new [3–5] (and not yet completely general). Since the formalism is rather involved, it is important to provide detailed checks that test all aspects of the approach.¹

The present work is aimed at extending previous tests of the formalism of Refs. [3–5] by considering the prediction of the quantization condition for a system of three identical scalar particles near threshold. These particles are confined to a cubic box of side L (as in a lattice simulation) and it is assumed that there is a Z_2 symmetry restricting interactions to those involving an even number of particles. The total momentum² is taken to be zero. Under these assumptions, Ref. [8] derived the expansion of the energy of the three-particle threshold state in powers of $1/L$, keeping terms up to $\mathcal{O}(1/L^6)$. This threshold expansion was derived for an arbitrary Z_2 -symmetric effective field theory. Unlike the two-particle case, where the derivation of the threshold expansion is rather straightforward, the derivation for three particles is itself very involved, requiring the summation of several infinite series. Thus the test presented here is a check of the derivation of the threshold expansion as well as of the underlying formalism.

The general formula for the threshold expansion is given in terms of infinite-volume quantities such as the two-particle scattering length. This result is tested here by calculating the same expansion in a specific Z_2 -symmetric theory— $\lambda\phi^4$ theory—and expressing the result in terms of the same infinite-volume quantities. This test has previously been passed at third order in λ , and through $\mathcal{O}(1/L^6)$ in the volume expansion, in Ref. [9], and what is presented here is the fourth-order calculation to the same order in $1/L$. The specific motivation for carrying out this lengthy and quite tedious calculation is that the fourth-order calculation tests qualitatively new aspects of the general prediction. Specifically, the general formalism contains a “divergence-free” three-particle scattering amplitude that is obtained from the three-to-three amplitude \mathcal{M}_3 by subtracting an infinite series of terms such that the physical singularities are removed. I stress that such singularities are inevitably present in \mathcal{M}_3 and must be dealt with. A simplified version of this subtraction procedure is sufficient at threshold [8], and defines a quantity called $\mathcal{M}_{3,\text{thr}}$. The $\mathcal{O}(\lambda^3)$ calculation did not test all the subtraction terms in the definition of $\mathcal{M}_{3,\text{thr}}$, but the present calculation does.

It turns out that, as part of the calculation of the three-particle threshold energy, one needs all the ingredients necessary to determine the two-particle threshold energy. Thus the latter energy can also be compared to the general result that follows from the formalism of Refs. [1, 2]. Since by now there is no doubt that this formalism is correct, this subsidiary calculation provides a check on the methods used here.

This paper is organized as follows. The following section contains a summary of the methods introduced in Ref. [9] to determine the threshold energy in perturbation theory, and presents the general results from Ref. [8] that are being tested. Section III concerns the two-particle energy shift, and provides a sketch of the calculation and the final results. These require the two-loop contribution to the effective range. Section IV describes the calculation of the contributions to the energy shift that are specific to three particles. This requires a particular off-shell version of the two-loop infinite-volume scattering amplitude, the calculation of which is similar to, but different from, that of the effective range. I conclude in Sec. V. Technical details are collected in three appendices: the first recalling some general results for finite-volume sums, the second listing the needed counterterms, and the third describing the calculation of the on- and off-shell two-loop scattering amplitude near threshold.

II. OVERVIEW OF METHODS AND RESULTS TO BE TESTED

The method I use is that introduced in Ref. [9], and I recall here only the essential features. The theory has the Euclidean Lagrangian density

$$\mathcal{L} = \frac{1}{2}\partial_\mu\phi\partial_\mu\phi + \frac{m^2}{2}\phi^2 + \frac{\lambda}{4!}\phi^4 + \frac{\delta Z}{2}\partial_\mu\phi\partial_\mu\phi + \frac{\delta Z_m}{2}m^2\phi^2 + \frac{\delta Z_\lambda}{4!}\phi^4, \quad (1)$$

with ϕ a scalar field. An on-shell renormalization scheme is used: δZ and δZ_m are tuned so that m is the physical mass and the residue of the (infinite-volume) propagator at the pole is unity. The counterterm δZ_λ is defined by the

¹ An alternative approach to the three-particle quantization condition was proposed very recently in Refs. [6, 7]. The threshold expansion in this new approach has not yet been derived.

² I use “momentum” for three-momentum throughout this work aside from in Appendix C.

requirement that the scattering amplitude at threshold is given by $-\lambda$ to all orders. Since this threshold amplitude is, by definition, proportional to the scattering length, a , this renormalization condition implies the exact relation

$$\lambda = 32\pi m a. \quad (2)$$

I will need the two-loop form of δZ_λ , and this is given in Appendix B.

The finite-volume (FV) energies are extracted from the long-time behavior of the following correlation functions:

$$C_2(\tau) = \frac{(2m)^2}{2L^6} e^{2m\tau} \left\langle \tilde{\phi}_{\vec{0}}(\tau)^2 \tilde{\phi}_{\vec{0}}(0)^2 \right\rangle, \quad (3)$$

$$C_3(\tau) = \frac{(2m)^3}{6L^9} e^{3m\tau} \left\langle \tilde{\phi}_{\vec{0}}(\tau)^3 \tilde{\phi}_{\vec{0}}(0)^3 \right\rangle. \quad (4)$$

Here τ is Euclidean time, which is always taken to be positive or zero, and the interpolating fields are

$$\tilde{\phi}_{\vec{p}}(\tau) = \int_L d^3x e^{-i\vec{p}\cdot\vec{x}} \phi(\vec{x}, \tau), \quad (5)$$

with the subscript L indicating that the integral is over the cubic box. Periodic boundary conditions are applied to ϕ , so that momenta are quantized as $\vec{p} = 2\pi\vec{n}/L$, with \vec{n} a vector of integers. Euclidean time is taken to have infinite range. The prefactors in Eqs. (3) and (4) are chosen so that $C_j(\tau) = 1$ for all τ if $\lambda = 0$. In this limit the interpolating operators couple to the states consisting of j particles at rest.

When $\lambda \neq 0$ the correlators behave as (recalling that $\tau \geq 0$)

$$C_j(\tau) = \sum_k A_{j,k} e^{-\Delta E_{j,k}\tau}, \quad \Delta E_{j,k} \equiv E_{j,k} - jm, \quad (6)$$

where $j = 2$ or 3 , k labels the finite-volume states that couple to the interpolators, and $A_{j,k}$ are the corresponding amplitudes. The state of interest is that nearest threshold for which $\Delta E_{j,k} \rightarrow 0$ as $\lambda \rightarrow 0$. This is labeled by $k = \text{thr}$. The procedure developed in Ref. [9] for picking out its energy is to first calculate $C_2(\tau)$ and $C_3(\tau)$ order by order in PT, then remove by hand exponentially growing or falling contributions. The resulting subtracted correlators have the form

$$C_{j,\text{thr}}(\tau) = C_{j,\text{thr}}(0) + \tau [\partial_\tau C_{j,\text{thr}}(0)] + \mathcal{O}(\tau^2). \quad (7)$$

Finally, the shift of the desired energy from threshold is given by

$$\Delta E_{j,\text{thr}} = -\frac{\partial_\tau C_{j,\text{thr}}(0)}{C_{j,\text{thr}}(0)}. \quad (8)$$

The justification for this method is explained in Ref. [9].

The perturbative expansions of the quantities appearing in this expression are³

$$C_{j,\text{thr}}(0) = 1 + \sum_{n=1}^{\infty} \lambda^n C_{j,\text{thr}}^{(n)}(0), \quad (9)$$

$$\partial_\tau C_{j,\text{thr}}(0) = \sum_{n=1}^{\infty} \lambda^n [\partial_\tau C_{j,\text{thr}}^{(n)}(0)], \quad (10)$$

$$\Delta E_{j,\text{thr}} = \sum_{n=1}^{\infty} \lambda^n \Delta E_{j,\text{thr}}^{(n)}. \quad (11)$$

Inserting these expansions into Eq. (8), the result for the fourth order term in $\Delta E_{j,\text{thr}}$ is

$$\begin{aligned} \Delta E_{j,\text{thr}}^{(4)} = & -\partial_\tau C_{j,\text{thr}}^{(4)}(0) + C_{j,\text{thr}}^{(1)}(0) [\partial_\tau C_{j,\text{thr}}^{(3)}(0)] + C_{j,\text{thr}}^{(2)}(0) [\partial_\tau C_{j,\text{thr}}^{(2)}(0)] + C_{j,\text{thr}}^{(3)}(0) [\partial_\tau C_{j,\text{thr}}^{(1)}(0)] \\ & - [C_{j,\text{thr}}^{(1)}(0)]^2 [\partial_\tau C_{j,\text{thr}}^{(2)}(0)] - 2C_{j,\text{thr}}^{(1)}(0) C_{j,\text{thr}}^{(2)}(0) [\partial_\tau C_{j,\text{thr}}^{(1)}(0)] + [C_{j,\text{thr}}^{(1)}(0)]^3 [\partial_\tau C_{j,\text{thr}}^{(1)}(0)]. \end{aligned} \quad (12)$$

³ Here I am expanding in the renormalized coupling, whereas the corresponding expansions in Ref. [9] were in powers of the bare coupling. For the sake of brevity, I continue to use the same notation for the expansion coefficients, although the values of these coefficients differ.

I calculate $\Delta E_{j,\text{thr}}^{(4)}$ only up to order $1/L^6$ in the volume expansion. From Ref. [9] the leading $1/L$ behavior of the terms in Eq. (12) is known to be

$$\begin{aligned} C_{j,\text{thr}}^{(2)}(0) &\sim 1/L^2, & C_{j,\text{thr}}^{(1)}(0) &\sim [\partial_\tau C_{j,\text{thr}}^{(1)}(0)] \sim 1/L^3, \\ [\partial_\tau C_{j,\text{thr}}^{(2)}(0)] &\sim 1/L^4, & [\partial_\tau C_{j,\text{thr}}^{(3)}(0)] &\sim 1/L^5. \end{aligned} \quad (13)$$

Explicit examples are given below. Thus the only contributions that must be kept are

$$\Delta E_{j,\text{thr}}^{(4)} = -\partial_\tau C_{j,\text{thr}}^{(4)}(0) + C_{j,\text{thr}}^{(2)}(0)[\partial_\tau C_{j,\text{thr}}^{(2)}(0)] + C_{j,\text{thr}}^{(3)}(0)[\partial_\tau C_{j,\text{thr}}^{(1)}(0)] + \mathcal{O}(1/L^7). \quad (14)$$

Since $C_{j,\text{thr}}^{(2)}(0)$, $[\partial_\tau C_{j,\text{thr}}^{(2)}(0)]$ and $[\partial_\tau C_{j,\text{thr}}^{(1)}(0)]$ are determined in Ref. [9], the only new quantities needed here are the $1/L^6$ contributions to $[\partial_\tau C_{j,\text{thr}}^{(4)}(0)]$ and the $1/L^3$ contributions to $C_{j,\text{thr}}^{(3)}(0)$. For both quantities these are the leading contributions in the $1/L$ expansion.

I now describe the results that I aim to check. The threshold expansion for the energy shift for two particles follows from the general formalism of Refs. [1, 2]. It is worked out through $\mathcal{O}(1/L^5)$ in Ref. [1] and the $1/L^6$ term is given in Ref. [9]. The result is

$$\Delta E_{2,\text{thr}} = \frac{4\pi a}{mL^3} \left\{ 1 - \left(\frac{a}{\pi L}\right) \mathcal{I} + \left(\frac{a}{\pi L}\right)^2 (\mathcal{I}^2 - \mathcal{J}) + \left(\frac{a}{\pi L}\right)^3 [-\mathcal{I}^3 + 3\mathcal{I}\mathcal{J} - \mathcal{K}] + \frac{2\pi r a^2}{L^3} - \frac{\pi a}{m^2 L^3} \right\} + \mathcal{O}(L^{-7}), \quad (15)$$

with a the scattering length (defined to be positive for repulsive interactions), r the effective range, and $\mathcal{I}, \mathcal{J}, \mathcal{K}$ are known sums over functions of integer vectors (see Appendix A). The result for the three-particle threshold energy is [8]⁴

$$\begin{aligned} \Delta E_{3,\text{thr}} = \frac{12\pi a}{mL^3} \left\{ 1 - \left(\frac{a}{\pi L}\right) \mathcal{I} + \left(\frac{a}{\pi L}\right)^2 (\mathcal{I}^2 + \mathcal{J}) + \frac{64\pi^2 a^2 \mathcal{C}_3}{mL^3} + \frac{3\pi a}{m^2 L^3} + \frac{6\pi r a^2}{L^3} \right. \\ \left. + \left(\frac{a}{\pi L}\right)^3 [-\mathcal{I}^3 + \mathcal{I}\mathcal{J} + 15\mathcal{K} + c_L \log(N_{\text{cut}}) + \mathcal{C}_F + \mathcal{C}_4 + \mathcal{C}_5] \right\} - \frac{\mathcal{M}_{3,\text{thr}}}{48m^3 L^6} + \mathcal{O}(L^{-7}), \quad (16) \end{aligned}$$

where $N_{\text{cut}} = mL/(2\pi)$, $c_L = 16\pi^3(\sqrt{3} - 4\pi/3)$, and $\mathcal{C}_F, \mathcal{C}_3, \mathcal{C}_4$ and \mathcal{C}_5 are sums over integer vectors that are defined and evaluated in Ref. [8]. The new amplitude entering at $\mathcal{O}(1/L^6)$ is the divergence-free three-to-three threshold amplitude $\mathcal{M}_{3,\text{thr}}$, which begins at $\mathcal{O}(\lambda^2)$ in perturbation theory. The numerical values of $\mathcal{C}_3, \mathcal{C}_4$ and \mathcal{C}_5 depend on the choice of UV cutoff, but this dependence cancels with that of $\mathcal{M}_{3,\text{thr}}$. This cancellation is necessary because $\Delta E_{3,\text{thr}}$ is a physical quantity.

Since a and λ are proportional [Eq. (2)], the dependence of $\Delta E_{j,\text{thr}}$ on λ is manifest except for the terms involving r and $\mathcal{M}_{3,\text{thr}}$. To make the perturbative expansion clearer I rewrite r , using its definition, as

$$32\pi m^3 r a^2 \equiv -\lambda - 2\mathcal{K}'_{2,s,\text{thr}}, \quad (17)$$

where

$$\mathcal{K}'_{2,s,\text{thr}} \equiv m^2 \frac{d\mathcal{K}_{2,s}}{dq^2} \Big|_{\text{thr}}, \quad (18)$$

Here $\mathcal{K}_{2,s}$ is the two-particle s-wave K matrix, and q is the momentum of each particle in the two-particle CM frame. The perturbative series for $\mathcal{K}'_{2,s,\text{thr}}$ and $\mathcal{M}_{3,\text{thr}}$ both begin at $\mathcal{O}(\lambda^2)$:

$$\mathcal{K}'_{2,s,\text{thr}} = \sum_{n=2}^{\infty} \lambda^n \mathcal{K}'_{2,s,\text{thr}}^{(n)}, \quad \mathcal{M}_{3,\text{thr}} = \sum_{n=2}^{\infty} \lambda^n \mathcal{M}_{3,\text{thr}}^{(n)}. \quad (19)$$

⁴ In the initial published version the coefficient of \mathcal{K} was -9 , but this was corrected in an Erratum to $+15$ [8].

Combining these results, the predictions above imply that the fourth-order terms are

$$\Delta E_{2,\text{thr}}^{(4)} = \frac{1}{2^{18}\pi^6 m^5 L^6} [-\mathcal{I}^3 + 3\mathcal{I}\mathcal{J} - \mathcal{K}] - \frac{\mathcal{K}'_{2,s,\text{thr}}(3)}{2^6 m^5 L^6} + \mathcal{O}(L^{-7}), \quad (20)$$

$$\Delta E_{3,\text{thr}}^{(4)} = \frac{3}{2^{18}\pi^6 m^5 L^6} [-\mathcal{I}^3 + \mathcal{I}\mathcal{J} + 15\mathcal{K} + c_L \log(N_{\text{cut}}) + \mathcal{C}_F + \mathcal{C}_4 + \mathcal{C}_5] - \frac{9\mathcal{K}'_{2,s,\text{thr}}(3)}{2^6 m^5 L^6} - \frac{\mathcal{M}_{3,\text{thr}}^{(4)}}{48m^3 L^6} + \mathcal{O}(L^{-7}). \quad (21)$$

In order to separate out effects that are particular to the three-particle case, it is convenient to consider the difference

$$\Delta_{32} = \Delta E_{3,\text{thr}} - 9\Delta E_{2,\text{thr}} = \sum_{n=2}^{\infty} \lambda^n \Delta_{32}^{(n)}, \quad (22)$$

for which the fourth-order coefficient is predicted to be

$$\Delta_{32}^{(4)} = \frac{3}{2^{18}\pi^6 m^5 L^6} [2\mathcal{I}^3 - 8\mathcal{I}\mathcal{J} + 18\mathcal{K} + c_L \log(N_{\text{cut}}) + \mathcal{C}_F + \mathcal{C}_4 + \mathcal{C}_5] - \frac{\mathcal{M}_{3,\text{thr}}^{(4)}}{48m^3 L^6} + \mathcal{O}(L^{-7}). \quad (23)$$

Note that the effective range has canceled from this expression.

To motivate the definition of Δ_{32} , I recall from Ref. [9] that the three-particle correlators can be split into a ‘‘connected’’ part, containing contributions in which the Feynman diagram connects all three particles, a ‘‘disconnected’’ part in which one particle is a spectator (possibly having self-energy insertions) and the other two are connected, and the fully disconnected remainder (which does not lead to power-law finite-volume effects). Since there are three possible two-particle pairs in a three-particle system, the following relations hold for all n ,

$$C_{3,\text{thr},\text{disc}}^{(n)}(0) = 3C_{2,\text{thr}}^{(n)}(0), \quad \partial_\tau C_{3,\text{thr},\text{disc}}^{(n)}(0) = 3\partial_\tau C_{2,\text{thr}}^{(n)}(0). \quad (24)$$

As noted in Ref. [9], for $n = 1$ and 2 , connected contributions to C_3 do not begin until $\mathcal{O}(1/L^6)$, so that

$$C_{3,\text{thr}}^{(n)}(0) = 3C_{2,\text{thr}}^{(n)}(0) + \mathcal{O}(L^{-6}) \quad (n = 1, 2). \quad (25)$$

while the low order contributions to the connected part of $C_{3,\text{thr}}^{(n)}(0)$ satisfy

$$\partial_\tau C_{3,\text{thr},\text{conn}}^{(1)}(0) = 0, \quad \partial_\tau C_{3,\text{thr},\text{conn}}^{(2)}(0) = \mathcal{O}(L^{-6}). \quad (26)$$

Combining these results yields

$$\Delta_{32}^{(4)} = -\partial_\tau C_{3,\text{thr},\text{conn}}^{(4)}(0) + 3C_{3,\text{thr},\text{conn}}^{(3)}(0)\partial_\tau C_{2,\text{thr}}^{(1)}(0) + 6\partial_\tau C_{2,\text{thr}}^{(4)}(0) + \mathcal{O}(L^{-7}). \quad (27)$$

showing that several two-particle quantities have canceled in the difference.

To summarize the previous discussion, the new quantities that are needed to determine $\Delta E_{3,\text{thr}}^{(4)}$ are $C_{2,\text{thr}}^{(3)}(0)$, $\partial_\tau C_{2,\text{thr}}^{(4)}(0)$, $\partial_\tau C_{3,\text{thr},\text{conn}}^{(3)}$ and $\partial_\tau C_{3,\text{thr},\text{conn}}^{(4)}$. Once these quantities have been calculated it requires no extra work to determine the result for $\Delta E_{2,\text{thr}}^{(4)}$. Having done so, it is convenient to consider $\Delta_{32}^{(4)}$ instead of $\Delta E_{3,\text{thr}}^{(4)}$. Breaking up the calculation in this way also proved useful in practice for tracking down errors.

The calculation of the finite-volume correlation functions proceeds as in Ref. [9]. Propagators are written in their time-momentum form, i.e. $\exp(-|\Delta t|\omega_p)/(2\omega_p)$ with $\omega_p = \sqrt{m^2 + p^2}$ and $p = |\vec{p}|$. The integrals over the vertex times, τ_i , are then straightforward but tedious.⁵ This leaves a sum over momenta of a summand that is, in general, quite complicated. For the sake of brevity, I do not display these summands except in a few cases.⁶ The sums are always UV finite after inclusion of counterterms. There are up to three loop-momenta in the diagrams considered.

At this stage the sums are replaced by integrals plus a volume-dependent difference. The general analysis of Refs. [1, 9, 10], implies that the sum-integral difference is exponentially suppressed in L (typically as e^{-mL}) except for loops in which intermediate particles can go on shell. Such loops have summands that diverge in the IR, and the results collected in Appendix A can be used to pull out the dominant volume dependence. What is left is a finite integral that is, in the present calculation, at most of two-loop order. Such integrals can easily be evaluated numerically. The tests presented here also requires a two-loop calculation of the scattering length and the three-particle subtracted threshold amplitude, $\mathcal{M}_{3,\text{thr}}$. These are infinite-volume quantities where the calculations are most easily done using standard momentum-space Feynman rules and dimensional regularization. The calculations are outlined in Appendix C.

⁵ I use Mathematica to do these integrals, and have found that doing more than two integrals at once can lead to incorrect results. Thus all integrals are done stepwise, with numerical checks at each stage.

⁶ Expressions for all integrands or summands are available upon request from the author.

III. DETERMINING $\Delta E_{2,\text{thr}}^{(4)}$.

In this section I calculate the λ^4 contribution to $\Delta E_{2,\text{thr}}$. Given the form of the expected answer, I write

$$\Delta E_{2,\text{thr}}^{(4)} = \frac{a_2^{(4)}}{2^{18}\pi^6 m^5 L^6} + \mathcal{O}(L^{-7}), \quad (28)$$

and quote results for $a_2^{(4)}$.

I begin by collecting results from Ref. [9] that are needed in order to evaluate $\Delta E_{2,\text{thr}}^{(4)}$ using Eq. (14):⁷

$$C_{2,\text{thr}}^{(1)}(0) = -\frac{1}{16m^3 L^3}, \quad \partial_\tau C_{2,\text{thr}}^{(1)}(0) = -\frac{1}{8m^2 L^3}, \quad (29)$$

$$C_{2,\text{thr}}^{(2)}(0) = \frac{\mathcal{I}}{2^8 \pi^2 m^3 L^4} + \mathcal{O}(L^{-6}), \quad \partial_\tau C_{2,\text{thr}}^{(2)}(0) = -\frac{\mathcal{J}}{2^{10} \pi^4 m^2 L^2} + \mathcal{O}(L^{-3}), \quad (30)$$

Using these results one can immediately determine the $C_{2,\text{thr}}^{(2)}(0)\partial_\tau C_{2,\text{thr}}^{(2)}(0)$ contribution in Eq. (14), leading to⁸

$$a_2^{(4)} \supset -IJ \quad (31)$$

What remains is to calculate $C_{2,\text{thr}}^{(3)}(0)$ and $\partial_\tau C_{2,\text{thr}}^{(4)}(0)$.

A. Calculating $C_{2,\text{thr}}^{(3)}(0)$

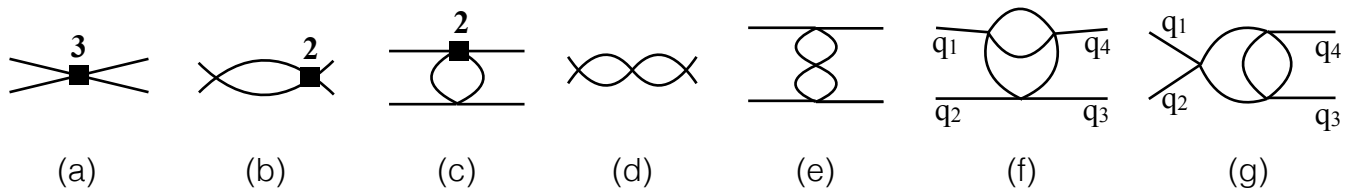


FIG. 1. Feynman diagrams contributing to $C_2(\tau)$ at $\mathcal{O}(\lambda^3)$. Solid squares are vertex counterterms, with the number indicating the power of λ . External particles have zero three-momentum. Diagrams related by vertical or horizontal reflection are not shown explicitly. Interpreted as contributions to the infinite-volume scattering amplitude, these are the diagrams required to calculate the two-loop counterterms in Appendix B, and the two-loop K matrix in Appendix C. The momentum labels in (f) and (g) are used in the latter calculation. Time runs from left to right in both applications.

The diagrams needed to calculate $C_{2,\text{thr}}^{(3)}(0)$ are shown in Fig. 1. Since $C_{2,\text{thr}}^{(3)}(0)$ appears in Eq. (14) multiplied by $\partial_\tau C_{2,\text{thr}}^{(1)}(0) = \mathcal{O}(L^{-3})$, $C_{2,\text{thr}}^{(3)}(0)$ itself is needed only up to $\mathcal{O}(L^{-3})$.

1. SS diagram

I begin by determining the contribution of Fig. 1(d), together with the A_{2s} contribution to Fig. 1(b), plus its horizontal reflection, and the A_{3ss} contribution to Fig. 1(a). I label the left- and right-hand loop momenta p and q , respectively. If both momenta vanish then the contribution is of $\mathcal{O}(L^{-9})$, well below the order of interest. Contributions of $\mathcal{O}(L^{-3})$ do arise, however, if one or both momenta are nonzero.

⁷ The results in Eq. (30) look different from those given in Eqs. (27) and (28) of Ref. [9] because here I expand in the renormalized rather than the bare coupling. In particular, terms proportional to A_2/L^3 present in Ref. [9] are canceled here by contributions from the $\mathcal{O}(\lambda^2)$ counterterm.

⁸ Here and in the following I use the proper superset symbol \supset to indicate individual contributions to quantities (with the quantity here being $a_2^{(4)}$). In the course of the calculation I determine all contributions of the desired order and collect them in a final result.

Consider first the case in which one momentum vanishes, say q . Then it is possible for all three time integrals to give factors of $1/p^2$, each arising from integrals of the form

$$\int_{\tau_i}^{\tau_k} d\tau_j e^{-(\tau_k - \tau_j)2(\omega_p - m)} \propto \frac{1 - e^{-(\tau_k - \tau_i)2(\omega_p - m)}}{2(\omega_p - m)} \sim \frac{1}{p^2}. \quad (32)$$

Explicit evaluation (including a factor of 2 from the fact that either loop momentum can vanish) yields

$$C_{2,\text{thr}}^{(3)}(0) \supset -\frac{1}{2^8 m^3 L^9} \sum_{\vec{p} \neq 0} \frac{1}{p^6} [1 + \mathcal{O}(p^2)] \quad (33)$$

$$= -\frac{\mathcal{K}}{2^{14} \pi^6 m^3 L^3} [1 + \mathcal{O}(L^{-1})], \quad (34)$$

Here I have kept only the most singular part of the summand, since less singular terms contribute at subleading order in L^{-1} . To obtain the second line I have used Eq. (A4). Note that, although a sum over p usually absorbs a single factor of L^{-3} (in order to become an integral), the presence of the $1/p^6$ IR divergence means that a factor of L^{-6} is absorbed. This brings the contribution up to the desired order.

If both loop momenta are nonvanishing, the summand is simple and so I display the complete result:

$$C_{2,\text{thr}}^{(3)}(0) \supset \frac{1}{2^9 m^3 L^3} \left\{ \frac{1}{L^3} \sum_{\vec{p} \neq 0} \frac{m^2}{\omega_p p^4} \left[\frac{1}{L^3} \sum_{\vec{q} \neq 0} - \int_q \right] \frac{1}{\omega_q q^2} + (p \leftrightarrow q) - \frac{1}{2} \left[\frac{1}{L^3} \sum_{\vec{p} \neq 0} - \int_p \right] \frac{1}{\omega_p p^2} \left[\frac{1}{L^3} \sum_{\vec{q} \neq 0} - \int_q \right] \frac{1}{\omega_q q^2} \right\} \quad (35)$$

$$= \frac{\mathcal{I}\mathcal{J}}{2^{14} \pi^6 m^3 L^3} [1 + \mathcal{O}(L^{-1})]. \quad (36)$$

To obtain the second line I have used Eqs. (A1) and (A2). Note that the maximal degree of IR divergence is the same as for when one momentum vanishes, but now the divergence is split between p and q . The final term in Eq. (35) has a lower degree of IR divergence, and gives a subleading contribution.

2. Remaining diagrams

The TT diagram, Fig. 1(e), combines with the A_{2t} contribution to Fig. 1(c), and the A_{3tt} contribution to Fig. 1(a). In this case, the absence of physical cuts allows the replacement of sums with integrals. The combined integrand, including counterterms, is UV and IR convergent:

$$C_{2,\text{thr}}^{(3)}(0) \supset -\frac{1}{2^{12} \pi^4 m^3 L^3} I^{\text{TT}}, \quad (37)$$

$$I^{\text{TT}} = 8\pi^4 \int_p \int_q \frac{m^3}{\omega_p^3 (\omega_p + m) \omega_q^3 (\omega_q + m) (\omega_p + \omega_q)} = \frac{2(\pi - 3)}{3}. \quad (38)$$

The SU diagram of Fig. 1(f) combines with the $A_{2s} + A_{2u}$ contribution to Fig. 1(c), and the A_{3su} contribution to Fig. 1(a). Again, sums can be replaced by integrals, leading to

$$C_{2,\text{thr}}^{(3)}(0) \supset -\frac{1}{2^9 \pi^4 m^3 L^3} I^{\text{SU}}, \quad I^{\text{SU}} = 0.0396563. \quad (39)$$

I only give the result of numerical integration, since the integrand is long and uninformative.

Finally, the ST diagram, Fig. 1(e), combines the $A_{2t} + A_{2u}$ contribution to Fig. 1(b), and the A_{3st} contribution to Fig. 1(a), together with their horizontal reflections. The total contribution only scales as $1/p^2$ in the IR, with no IR divergence in q . Thus both sums can be replaced by integrals up to corrections of relative size L^{-1} , leading to

$$C_{2,\text{thr}}^{(3)}(0) \supset -\frac{I^{\text{ST}}}{2^9 \pi^4 m^3 L^3}, \quad I^{\text{ST}} = 0.099447. \quad (40)$$

3. Total contribution to $\Delta E_{2,\text{thr}}^{(4)}$

Multiplying the above results by $\partial_\tau C_{2,\text{thr}}^{(1)}(0)$ from Eq. (29) yields

$$a_2^{(4)} \supset -2\mathcal{I}\mathcal{J} + 2\mathcal{K} + 2^6 \pi^2 (I^{\text{ST}} + \frac{1}{8} I^{\text{TT}} + I^{\text{SU}}). \quad (41)$$

B. Contribution of $\partial_\tau C_{2,\text{thr}}^{(4)}(0)$

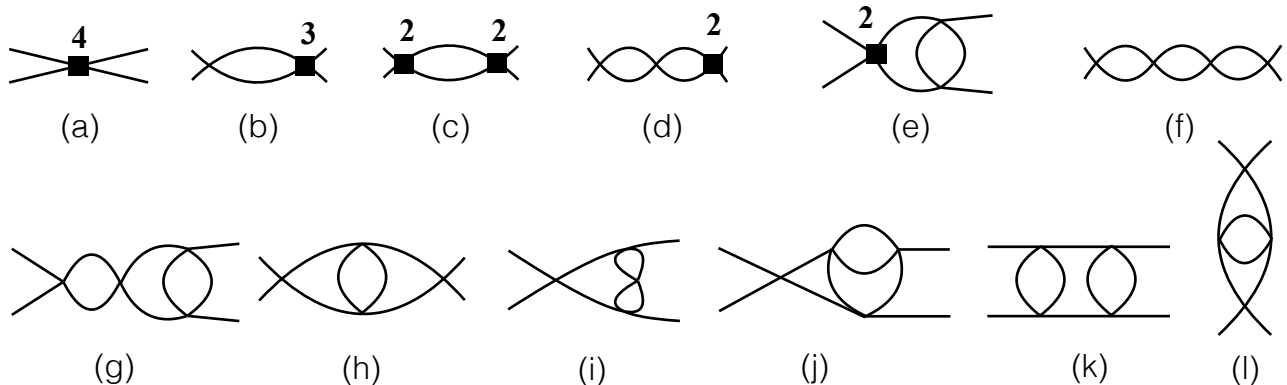


FIG. 2. Subset of Feynman diagrams contributing $C_2(\tau)$ at $\mathcal{O}(\lambda^4)$. Notation as in Fig. 1. Figures (b)-(k) show all the diagrams (aside from reflections, and additional placements of counterterms) for which there is a two-particle cut. Figure (l) shows a single example of the many diagrams without such cuts. See text for further discussion.

In this section I calculate the contribution to $a_2^{(4)}$ from $\partial_\tau C_{2,\text{thr}}^{(4)}(0)$. A large number of diagrams contribute to $\partial_\tau C_{2,\text{thr}}^{(4)}(0)$, a subset of which is shown in Fig. 2. I first describe some general properties of the contributions of these diagrams *if all loop momenta are nonzero*. In this case, a term linear in τ arises only from a configuration in which all vertices lie close in time and are integrated as a group over the full time interval. Configurations in which some vertices are separated by $\mathcal{O}(\tau)$ are exponentially suppressed. Thus the contribution to $\partial_\tau C_{2,\text{thr}}^{(4)}(0)$ arises from two particles at rest propagating freely between 0 and τ , except for a single quasi-local interaction. From this one can show that, as $L \rightarrow \infty$, the leading volume dependence of $\partial_\tau C_{2,\text{thr}}^{(4)}(0)$ has the form $c/(8m^2 L^3)$, where c is the contribution of the diagram (now viewed as an infinite-volume scattering diagram) to the scattering amplitude at threshold, $\mathcal{M}_{2,\text{thr}}$.⁹ Note that, when taking the $L \rightarrow \infty$ limit, all sums are replaced by integrals, $(1/L^3) \sum_{\vec{p}} \rightarrow \int_p$.

This result has two important consequences. The first is practical: it allows the determination of the integrand of $\mathcal{M}_{2,\text{thr}}$ from the summand appearing in $\partial_\tau C_{2,\text{thr}}^{(4)}(0)$ on a diagram by diagram basis. The prescription is simply to multiply the summand by $8m^2 L^{12}$. Here the factor of $8m^2 L^3$ noted above is multiplied by L^9 due to the conversion of three momentum sums into integrals. I use this result to calculate the counterterms quoted in Appendix B.

The second consequence is that the constant c vanishes when each three-loop diagram is combined with the corresponding counterterms. This is because the $\mathcal{O}(\lambda^4)$ contributions to $\mathcal{M}_{2,\text{thr}}$ vanish in the renormalization scheme I use. (Indeed, the only contribution is of $\mathcal{O}(\lambda)$.) Since c is obtained by replacing momentum sums with integrals, it follows that all finite-volume corrections arise from sum-integral differences. I stress again that this argument holds for the case in which all loop momenta are nonvanishing.

From this result follows a key simplification in the calculation of $\partial_\tau C_{2,\text{thr}}^{(4)}(0)$: only diagrams containing two-particle cuts can contribute. These are the diagrams shown in Fig. 2(f)-(k). For diagrams without such cuts, such as Fig. 2(l), sum-integral differences are exponentially suppressed and do not lead to power law volume dependence. Furthermore, for diagrams without cuts, the cases in which loop momenta vanish do not require separate consideration, as there are no IR divergences.

For the diagrams with two-particle cuts, one must also consider the cases in which one or more loop momenta vanish. In these cases the summands are not related to integrands of $\mathcal{M}_{2,\text{thr}}$, do not vanish, and must be calculated explicitly. If one loop momentum vanishes, then the contribution is of $\mathcal{O}(L^{-6})$ if the other loop sums are replaced by integrals.¹⁰ If two loop momenta vanish then the contribution begins at $\mathcal{O}(L^{-9})$ and can only be raised to the desired L^{-6} behavior if there is a $1/p^6$ IR divergence. This only occurs for Fig. 2(f). If all three loop momenta vanish, then the contribution is of $\mathcal{O}(L^{-12})$ and can be dropped.

⁹ Indeed, this is exactly the form that arises at tree level, where $\lambda \partial_\tau C_{2,\text{thr}}^{(1)}(0) = -\lambda/(8m^2 L^3)$.

¹⁰ It is possible in principle that IR divergences could reduce the power of $1/L$, but this does not occur in practice.

I now consider Figs. 2(f)-(k) in turn, calling them, respectively, the SSS, SST, STS, STT, SSU and TST diagrams.

1. SSS diagram

Figure. 2(f) combines with the A_{4sss} part of Fig. 2(a), the A_{3ss} part from Fig. 2(b), the A_{2s}^2 part from Fig. 2(c) and the A_{2s} part from Fig. 2(d). I find

$$\partial_\tau C_{2,\text{thr}}^{(4)}(0) \supset \frac{\mathcal{I}^3 - 6\mathcal{I}\mathcal{J} + 3\mathcal{K}}{2^{18}\pi^6 m^5 L^6}, \quad (42)$$

with the three terms arising, respectively, from having zero, one and two nonzero loop momenta.

2. SST diagram

Next I consider Fig. 2(g), together with the A_{4sst} contribution to Fig. 2(a), the A_{3st} contribution to Fig. 2(b), the $A_{2s}(A_{2t} + A_{2u})$ contribution to Fig. 2(c), the $A_{2t} + A_{2u}$ contribution to Fig. 2(d), and the A_{2s} contribution to Fig. 2(e).

The sum over the momenta in the rightmost loop can always be converted to an integral since the summand is non-singular. Thus at most one of the remaining loops can have vanishing momenta. I describe the calculations in some detail.

If all three loop momenta are nonvanishing, contributions arise from (a) a sum-integral difference on the left loop (with the other loops integrated), (b) a sum-integral difference on the central loop (with other loops integrated), and (c) sum-integral differences on left and central loops (with the rightmost loop integrated). I find by explicit calculation that the summands/integrands for the first two cases vanish identically. The explicit expression for case (c) is (including the horizontal reflection):

$$\partial_\tau C_{2,\text{thr}}^{(4)}(0) \supset \frac{1}{2^{10}L^3} \left\{ \left[\frac{1}{L^3} \sum_{\vec{p} \neq 0} - \int_p \right] \frac{1}{\omega_p p^2} \right\} \left\{ \left[\frac{1}{L^3} \sum_{\vec{k} \neq 0} - \int_k \right] \frac{1}{\omega_k k^2} \int_q \frac{f^{\text{SST}}(\vec{k}, \vec{q})}{\omega_q^3} \right\}, \quad (43)$$

$$f^{\text{SST}}(\vec{k}, \vec{q}) = -1 + \frac{2\omega_q^2(\omega_k + W_{qk})}{\omega_{qk}(W_{qk}^2 - 1)}, \quad (44)$$

where $W_{qk} = \omega_q + \omega_k + \omega_{qk}$ and $\omega_{qk}^2 = m^2 + (\vec{q} + \vec{k})^2$. A key result is that $f^{\text{SST}}(0, \vec{q}) = 0$. Using Eq. (A1), one sees that the expression in the left-hand curly braces is proportional to $1/L$, while that in the right-hand curly braces is proportional to $1/L^3$, so that the overall contribution to $\partial_\tau C_{2,\text{thr}}^{(4)}(0)$ is proportional to $1/L^7$ and can be dropped.

If the leftmost loop momentum vanishes, it turns out the the central loop has an integrable $1/k^2$ IR divergence. Replacing the central momentum sum with an integral [valid up to corrections of $\mathcal{O}(L^{-1})$], and including the horizontal reflection, yields the result

$$\partial_\tau C_{2,\text{thr}}^{(4)}(0) \supset \frac{I^{\text{SST0}}}{2^{13}\pi^4 m^5 L^6}, \quad I^{\text{SST0}} = 0.19889. \quad (45)$$

Here I^{SST0} is a UV convergent two-loop integral of a lengthy expression that I evaluate numerically. I note that the relation $I^{\text{SST0}} = 2I^{\text{ST}}$ holds numerically.

If the central loop momentum vanishes, then, if the left-hand momentum sum is replaced by an integral, the result vanishes identically. It follows that there is no $\mathcal{O}(L^{-6})$ contribution to $\partial_\tau C_{2,\text{thr}}^{(4)}(0)$.

3. STS diagram

Figure 2(h), combines with the Fig. 2(d) (in which the $A_{2t} + A_{2u}$ counterterm is placed on the middle vertex), as well as the A_{3st} contribution to Fig. 2(b) (together with its reflection) and the A_{4sts} contribution to Fig. 2(a).

The central loop sum can always be converted to an integral without power-law volume corrections. If both of the outer loop momenta are nonzero, I find (with \vec{p} and \vec{k} the momenta in the outer loops, and \vec{q} the central momentum)

$$\begin{aligned} \partial_\tau C_{2,\text{thr}}^{(4)}(0) \supset & \frac{1}{2^{11}m^2L^3} \left[\frac{1}{L^3} \sum_{\vec{p} \neq 0} - \int_p \right] \left[\frac{1}{L^3} \sum_{\vec{k} \neq 0} - \int_k \right] \frac{1}{\vec{p}^2 \vec{k}^2} \int_q f^{\text{STS1}}(\vec{p}, \vec{k}, \vec{q}) \\ & + \frac{1}{2^{10}m^2L^3} \left[\frac{1}{L^3} \sum_{\vec{p} \neq 0} - \int_p \right] \frac{1}{\vec{p}^2} \int_k \int_q f^{\text{STS2}}(\vec{p}, \vec{k}, \vec{q}). \end{aligned} \quad (46)$$

The relevant properties of the functions f^{STS1} and f^{STS2} will be given below. To study the first term in Eq. (46), I introduce

$$g^{\text{STS1}}(\vec{p}^2, \vec{k}^2, \vec{p} \cdot \vec{k}) = \int_q f^{\text{STS1}}(\vec{p}, \vec{k}, \vec{q}), \quad (47)$$

where the form of the arguments of $g^{(\text{STS1})}$ is determined by rotation invariance. Generalizing the analysis leading to Eq. (A1) gives

$$\left[\frac{1}{L^3} \sum_{\vec{p} \neq 0} - \int_p \right] \left[\frac{1}{L^3} \sum_{\vec{k} \neq 0} - \int_k \right] \frac{g(\vec{p}^2, \vec{k}^2, \vec{p} \cdot \vec{k})}{\vec{p}^2 \vec{k}^2} = \left(\frac{\mathcal{I}}{4\pi^2 L} \right)^2 g(0, 0, 0) - \frac{\mathcal{I}}{4\pi^2 L^4} \left[\frac{\partial}{\partial p^2} + \frac{\partial}{\partial k^2} \right] g \Big|_{\vec{p}=\vec{k}=0} + \mathcal{O}(1/L^6). \quad (48)$$

Using the result $g^{\text{STS1}}(0, 0, 0) = 0$, which follows from the renormalization condition, I find that the leading finite-volume term is proportional to L^{-7} .

Turning to the second term in Eq. (46), I introduce

$$g^{\text{STS2}}(\vec{p}^2) = \int_k \int_q f^{\text{STS2}}(\vec{p}, \vec{k}, \vec{q}), \quad (49)$$

which is a function of \vec{p}^2 by rotation invariance. Using

$$g^{\text{STS2}}(0) = 0, \quad g^{\text{STS2}'}(0) = \frac{I^{\text{STS}}}{8m^3\pi^4}, \quad I^{\text{STS}} = -0.37115, \quad (50)$$

together with Eq. (A1), the second term in Eq. (46) contributes

$$\partial_\tau C_{2,\text{thr}}^{(4)}(0) \supset \frac{-I^{\text{STS}}}{2^{13}\pi^4 m^5 L^6}. \quad (51)$$

If one or other of the outer momenta vanishes, then I find

$$\partial_\tau C_{2,\text{thr}}^{(4)}(0) \supset \frac{I^{\text{STS0}}}{2^{13}\pi^4 m^5 L^6}, \quad I^{\text{STS0}} = I^{\text{SST0}}, \quad (52)$$

where the latter equality holds to numerical precision.

4. STT diagram

Figure 2(i) combines with the A_{2t} contribution to Fig. 2(e) (with the counterterm on the two right-hand vertices), the A_{3tt} contribution to Fig. 2(b) and the A_{4stt} contribution to Fig. 2(a).

The sums over momenta in the right-hand loops can be converted to integrals. If no loop momenta vanish then the result, including the horizontal reflection, is

$$\partial_\tau C_{2,\text{thr}}^{(4)}(0) \supset \frac{1}{2^{10}m^3L^3} \left[\frac{1}{L^3} \sum_{p \neq 0} - \int_p \right] \frac{f^{\text{STT}}(p^2)}{p^2}, \quad (53)$$

$$f^{\text{STT}}(0) = 0, \quad f^{\text{STT}'}(0) = \frac{I^{\text{TT}}}{32\pi^4}. \quad (54)$$

Using Eq. (A1), this yields

$$\partial_\tau C_{2,\text{thr}}^{(4)}(0) \supset -\frac{I^{\text{TT}}}{2^{15}\pi^4 m^5 L^6}. \quad (55)$$

If the lefthand loop momentum vanishes, I find

$$\partial_\tau C_{2,\text{thr}}^{(4)}(0) \supset \frac{I^{\text{TT}}}{2^{14}\pi^4 m^5 L^6}, \quad (56)$$

with I^{TT} given in Eq. (38).

5. SSU diagram

Figure 2(j) combines with the $A_{2s} + A_{2u}$ contributions on the right-hand vertices in Fig. 2(e), the A_{3su} contribution to in Fig. 2(b) and the A_{4ssu} counterterm in Fig. 2(a). The fact that A_{2u} contributes is not obvious but can be understood by a careful accounting of the Wick contractions. Momentum sums in the two right-hand loops can be replaced by integrals. I label the momenta in these loops q and k , while that in the left-hand loop is denoted p . This is the most tedious of the diagrams to calculate.

If $\vec{p} \neq 0$ then the contribution takes the form

$$\partial_\tau C_{2,\text{thr}}^{(4)}(0) \supset \frac{1}{2^8 m^5 L^3} \left[\frac{1}{L^3} \sum_{\vec{p} \neq 0} - \int_p \right] \frac{1}{p^2} \int_{q,k} g^{\text{SSU}}(\vec{p}, \vec{q}, \vec{k}). \quad (57)$$

Using the fact that g^{SSU} vanishes when $\vec{p} = 0$ (which again follows from the renormalization condition), expanding g^{SSU} in powers of \vec{p} , and using Eq. (A1), I find

$$\partial_\tau C_{2,\text{thr}}^{(4)}(0) = -\frac{1}{2^{11}\pi^4 m^5 L^6} I^{\text{SSU}}, \quad I^{\text{SSU}} = 0.156906. \quad (58)$$

If $\vec{p} = 0$, the result is

$$\partial_\tau C_{2,\text{thr}}^{(4)}(0) = \frac{1}{2^{11}\pi^4 m^5 L^6} I^{\text{SU}}. \quad (59)$$

where I^{SU} is given in Eq. (39).

6. TST diagram

The final diagram is the box-like Fig. 2(k), which is combined with the $A_{2t} + A_{2u}$ contribution to Fig. 2(e), and the $(A_{2t} + A_{2u})^2$ contribution to Fig. 2(c).

The sums over the outer momenta can be replaced by integrals. If the central loop momentum (denoted \vec{p}) is nonvanishing, I find

$$\partial_\tau C_{2,\text{thr}}^{(4)}(0) \supset \frac{1}{2^{10} m^5 L^3} \left[\frac{1}{L^3} \sum_{p \neq 0} - \int_p \right] \frac{f^{\text{TST}}(p^2)}{p^2}, \quad (60)$$

$$f^{\text{TST}}(0) = 0, \quad f^{\text{TST}'} = \frac{I^{\text{TT}}}{32\pi^4}. \quad (61)$$

Using Eq. (A1) then yields

$$\partial_\tau C_{2,\text{thr}}^{(4)}(0) \supset -\frac{I^{\text{TT}}}{2^{15} m^5 L^6}. \quad (62)$$

If $\vec{p} = 0$, the result is

$$\partial_\tau C_{2,\text{thr}}^{(4)}(0) \supset \frac{I^{\text{TT}}}{2^{15} m^5 L^6}. \quad (63)$$

Thus the total contribution from this diagram vanishes.

7. Total contribution to $\Delta E_{2,\text{thr}}^{(4)}$

Combining the results from Eqs. (42), (45), (51), (52), (55), (56), (58), (59), (62) and (63), I obtain

$$a_2^{(4)} \supset -\mathcal{I}^3 + 6\mathcal{I}\mathcal{J} - 3\mathcal{K} - 2^5\pi^2 (I^{\text{SST}0} - I^{\text{ST}} + I^{\text{STS}} + I^{\text{STS}0} + \frac{1}{4}I^{\text{TT}} - 4I^{\text{SSU}} + 4I^{\text{SU}}) . \quad (64)$$

C. Mass and wavefunction renormalization

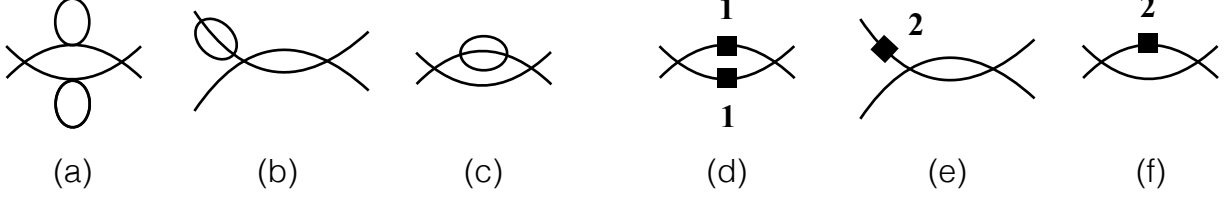


FIG. 3. Examples of Feynman diagrams contributing to $\partial_\tau C_{2,\text{thr}}^{(4)}(0)$ involving mass and wavefunction renormalization subdiagrams. Mass and wavefunction counterterms are indicated by filled boxes.

Both $C_{2,\text{thr}}^{(3)}(0)$ and $\partial_\tau C_{2,\text{thr}}^{(4)}(0)$ receive contributions from many diagrams involving mass and wavefunction renormalization parts. Examples are shown in Fig. 3. In all cases loop sums can be replaced by integrals. As explained in Ref. [9], tadpole bubbles, such as those in Fig. 3(a), cancel identically with the corresponding counterterms, here shown in Fig. 3(d). For loop diagrams such as those in Figs. 3(b) and (c), however, the cancelation with the counterterms of Figs. 3(e) and (f), is not exact. When one constructs the renormalized propagator by the usual geometric sum, what remains are contact terms in position space. These, however, cannot go on shell, and thus cannot be cut, so loops involving them do not lead to finite-volume dependence. Instead, they either lead to contributions to the amplitudes $A_{j,k}$ [see Eq. (6)] which thus cancel from ΔE_2 —exemplified by the case of Fig. 3(b)—or their contribution is canceled by coupling-constant counterterms—as is the case for Fig. 3(c). I have checked this explicitly for several examples. The net result is that this class of diagrams does not need to be considered.

D. Total result and comparison with expectation

Combining the results in Eqs. (31), (41) and (64) gives the final result for the two-particle energy shift

$$a_2^{(4)} = -\mathcal{I}^3 + 3\mathcal{I}\mathcal{J} - \mathcal{K} - 2^5\pi^2 (I^{\text{SST}0} - 2I^{\text{ST}} - I^{\text{STS}} + I^{\text{STS}0} - 4I^{\text{SSU}} + 2I^{\text{SU}}) . \quad (65)$$

This should be compared to the result expected from the quantization condition, Eq. (20), which yields

$$a_2^{(4)} = -\mathcal{I}^3 + 3\mathcal{I}\mathcal{J} - \mathcal{K} - 2^{12}\pi^6 \mathcal{K}'_{2,s,\text{thr}}{}^{(3)} . \quad (66)$$

The coefficients of the geometric constants agree. For the remaining part the result for $\mathcal{K}'_{2,s,\text{thr}}{}^{(3)}$ from Appendix C is needed. Combining Eqs. (C19) and (C24), the result is

$$\mathcal{K}'_{2,s,\text{thr}}{}^{(3)} = \frac{I^{\text{STr}}}{2^8\pi^4} + \frac{I^{\text{SUr}}}{2^6\pi^4} . \quad (67)$$

Agreement between Eqs. (65) and (66) holds because of the numerical relations

$$I^{\text{SST}0} - 2I^{\text{ST}} - I^{\text{STS}} + I^{\text{STS}0} = \frac{1}{2}I^{\text{STr}} , \quad (68)$$

$$-4I^{\text{SSU}} + 2I^{\text{SU}} = 2I^{\text{SUr}} . \quad (69)$$

From the point of view of the present calculation this agreement appears highly nontrivial, as the two sides of these equations are obtained in very different ways. I stress that the agreement holds separately for subsets of diagrams: the

SSU contribution to $\partial_\tau C_{2,\text{thr}}^{(4)}(0)$, combined with the SU contribution to $C_{2,\text{thr}}^{(3)}(0)\partial_\tau C_{2,\text{thr}}^{(1)}(0)$ matches with to $\mathcal{K}'_{2,s,\text{thr}}{}^{(3, su)}$, while the SST and STS contributions to $\partial_\tau C_{2,\text{thr}}^{(4)}(0)$, combined with the ST contribution to $C_{2,\text{thr}}^{(3)}(0)\partial_\tau C_{2,\text{thr}}^{(1)}(0)$, matches with $\mathcal{K}'_{2,s,\text{thr}}{}^{(3, st)}$. This diagram-level matching holds also for the SSS, STT and TST classes of diagrams, where there is no contribution to $\mathcal{K}'_{2,s,\text{thr}}{}^{(3)}$.

IV. DETERMINING $\Delta_{32}^{(4)}$

In this section I calculate $\Delta_{32}^{(4)}$ in order to test the result (27) obtained from the three-particle quantization condition. It is convenient to write

$$\Delta_{32}^{(4)} = \frac{3a_3^{(4)}}{2^{18}\pi^6 m^5 L^6} + \mathcal{O}(L^{-7}), \quad (70)$$

and quote results for $a_3^{(4)}$. As shown in Eq. (23), the calculation requires determining $\partial_\tau C_{2,\text{thr}}^{(4)}(0)$, $C_{3,\text{thr,conn}}^{(3)}(0)$ and $\partial_\tau C_{3,\text{thr,conn}}^{(4)}$. The former was worked out in Sec. IIIB, and from Eq. (64) I find

$$a_3^{(4)} \Big|_{\partial_\tau C_{2,\text{thr}}^{(4)}(0)} = 2\mathcal{I}^3 - 12\mathcal{I}\mathcal{J} + 6\mathcal{K} + 2^6\pi^2 (I^{\text{SST0}} + I^{\text{STS0}} - I^{\text{STS}} + \frac{1}{4}I^{\text{TT}} + 4I^{\text{SU}} - 4I^{\text{SSU}}). \quad (71)$$

In the following two subsections I calculate the other two required quantities.

A. Calculation of $C_{3,\text{thr,conn}}^{(3)}(0)$

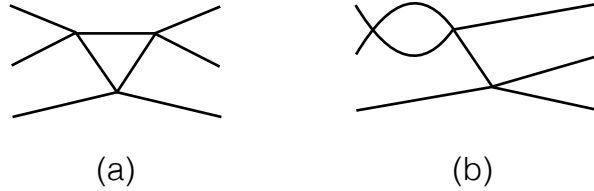


FIG. 4. Feynman diagrams for $C_{3,\text{thr,conn}}^{(3)}(0)$ that give contributions of $\mathcal{O}(L^{-3})$.

In order to give rise to an $\mathcal{O}(L^{-6})$ contribution to $\Delta_{32}^{(4)}$, $C_{3,\text{thr,conn}}^{(3)}(0)$ must scale as L^{-3} . Since connected diagrams begin at $\mathcal{O}(1/L^6)$, to reach the required dependence requires a $1/p^6$ IR divergence. This is only possible in third order diagrams if there is a time ordering of vertices in which all intermediate states contain only three particles (for each such intermediate state can yield a factor of $1/p^2$). This singles out the two diagrams shown in Fig. 4, which I denote, following Ref. [9], as (a) the bull's head and (b) the s-channel fish diagram.

The calculation is very straightforward as only one time-ordering is required. The contribution from the bull's head diagram is

$$C_{3,\text{thr,conn}}^{(3)}(0) \supset -\frac{3}{2^7 m^3 L^9} \sum_{\vec{p} \neq 0} \frac{-2 + \mathcal{O}(p^2)}{p^6} = \frac{3}{2^{13}\pi^6 m^3 L^3} (2\mathcal{K}) + \mathcal{O}(1/L^4), \quad (72)$$

while that from the s-channel fish (together with its horizontal reflection) is

$$C_{3,\text{thr,conn}}^{(3)}(0) \supset -\frac{3}{2^7 m^3 L^9} \sum_{\vec{q} \neq 0} \frac{1 + \mathcal{O}(q^2)}{q^6} = \frac{3}{2^{13}\pi^6 m^3 L^3} (-\mathcal{K}) + \mathcal{O}(1/L^4). \quad (73)$$

In both cases I have used Eq. (A4). Combining these results and multiplying by $3\partial_\tau C_{2,\text{thr}}^{(1)}(0)$ yields

$$a_3^{(4)} \Big|_{C_{3,\text{thr,conn}}^{(3)}(0)} = -12\mathcal{K}. \quad (74)$$

B. Calculation of $\partial_\tau C_{3,\text{thr,conn}}^{(4)}$

At $\mathcal{O}(\lambda^4)$, connected three-particle diagrams contain two loops. A selection of the many such diagrams is shown in Figs. 5, 6 and 7, including the subset that will need to be considered in detail. As for $\partial_\tau C_{2,\text{thr}}^{(4)}(0)$, the diagrams have an initial volume scaling of L^{-12} . This can be raised to the desired L^{-6} dependence either by converting two sums over intermediate momenta to integrals or by having a single loop sum that diverges in the IR as $1/p^6$. The latter case requires that the second loop momentum vanishes.¹¹ As already noted above, to obtain the most singular IR divergence the diagram must be such that there is a time ordering in which all intermediate states involve three particles. The diagrams for which this holds are Figs. 5(a), (d) and (g), Fig. 6(a) and Fig. 7(a).

If both loop momenta vanish then the contributions are proportional to $1/L^{12}$ and thus of too high order.

When both loop momenta are nonzero, there are two further general results that simplify the calculations. The first is that, as for $\partial_\tau C_{2,\text{thr}}^{(4)}(0)$, the vertex times, τ_i , must satisfy $0 < \tau_i < \tau$. The second concerns the summand that remains after the time integrals are done (leaving only momentum sums). For $\partial_\tau C_{2,\text{thr}}^{(4)}(0)$, this summand was proportional to the integrand of \mathcal{M}_2 at threshold. Here, by a similar argument, one can show that the summand of a contribution to $\partial_\tau C_{3,\text{thr,conn}}^{(4)}$, when multiplied by $48m^3L^{12}$, gives the integrand of \mathcal{M}_3 at threshold.¹² This implies that if both loop sums can be replaced by integrals, which is allowed in the absence of IR divergences, then the diagram will give a contribution of the form¹³

$$\partial_\tau C_{3,\text{thr,conn}}^{(4)} \supset \frac{\mathcal{M}_{3,\text{thr}}}{48m^3L^6} + \mathcal{O}(L^{-7}). \quad (75)$$

I will refer to this as the ‘‘standard form’’ of contribution.

Thus the only diagrams that need to be considered in detail are those containing IR divergences. These arise when the diagram has three-particle cuts. Thus, for example, Fig. 5(b) need not be considered, since it has no three-particle cuts and thus contributes only to the standard form, Eq. (75). All diagrams having three-particle cuts are included in Figs. 5, 6 and 7, with the exception of those with self-energy insertions or that are one-particle reducible. The latter do not lead to nonstandard contributions and are discussed in Sec. IV C.

A further distinction allows a subset of the diagrams with three-particle cuts to be removed from consideration. If the IR divergence occurs inside a loop, then it must be stronger than $1/p^2$ in order for Eq. (75) to be invalidated, as such an IR divergence is integrable. Since each three-particle cut only leads to a $1/p^2$ divergence, this implies that, for diagrams in which the three-particle cuts run through loops, there must be at least two such cuts if in order to obtain a result different from Eq. (75). Thus Fig. 5(c) need not be considered. The alternative is that the single three-particle cut does not pass through a loop, which is the case for Fig. 6(c) and Figs. 6(d), (e) and (f). These diagrams can lead to contributions of a form differing from Eq. (75) and must be considered in detail.

The final general issue arises from the fact that \mathcal{M}_3 at threshold is IR divergent and thus ill-defined. This is not the case for \mathcal{M}_2 , and adds another level of complication to the three-particle analysis. To obtain a well-defined three-particle amplitude at threshold one must add an IR regulator, make some subtractions, and then remove the regulator [3]. The choice of subtraction introduces scheme dependence, and a particularly simple choice was introduced in Ref. [8] and used to define the quantity $\mathcal{M}_{3,\text{thr}}$ that occurs in the prediction that I am testing, Eq. (23). The general implication is that, for diagrams with IR divergences that are not integrable, one must determine both their contributions to $\partial_\tau C_{3,\text{thr,conn}}^{(4)}$ and, in a separate infinite-volume calculation, to $\mathcal{M}_{3,\text{thr}}$, so that the deviation from the standard result (75) can be found. In the following I work systematically through all such diagrams carrying out this procedure.

It will be useful to have in mind the form of the IR subtractions that are needed. These are defined in Eq. (114) of Ref. [8] and the subsequent text. The schematic form is

$$\mathcal{M}_{3,\text{thr}} \equiv \lim_{\delta \rightarrow 0} \left\{ \mathcal{M}_{3,\delta} - I_{0,\delta} - \int_{k_{1,\delta}} \Xi_1(\vec{k}_1) - \int_{k_{1,\delta}} \int_{k_{2,\delta}} \Xi_2(\vec{k}_1, \vec{k}_2) \right\}. \quad (76)$$

Here δ is an IR regulator defined such that threshold is attained when $\delta \rightarrow 0$. The specific form of this regulator, as well as the explicit expressions for $I_{0,\delta}$, Ξ_1 and Ξ_2 , will be given below when needed. $I_{0,\delta}$ contains terms of all orders

¹¹ This is the most IR singular summand possible at this order because, of the four integrals over the times of the vertices, one is needed to produce the factor of τ , while each of the other three can lead to a factor of $1/p^2$.

¹² The factor of 48 can be understood from the case of a local $\lambda_6\phi^6/6!$ interaction, for which $\mathcal{M}_3 = -\lambda_6$. The contribution to $\partial_\tau C_{3,\text{thr,conn}}^{(4)}$ is then $-\lambda_6/[6(2m)^3]$, with the 6 arising from the numerator in ratio defining $\partial_\tau C_{3,\text{thr}}^{(4)}(0)$, Eq. (4), and the $(2m)^{-3}$ arising from the three propagators that are not canceled in this ratio.

¹³ In the remainder of this section the fact that there are contributions of $\mathcal{O}(L^{-7})$ will not be noted explicitly.

in λ starting at λ^2 , while Ξ_1 contains terms proportional to λ^3 and λ^4 , and Ξ_2 is proportional to λ^4 . Thus several new features of the subtraction scheme are being tested by working at $\mathcal{O}(\lambda^4)$. I also note that $I_{0,\delta}$ is used to subtract IR divergences in the diagrams of Figs. 6 and 7, while Ξ_1 and Ξ_2 are needed for some of the diagrams in Fig. 5.

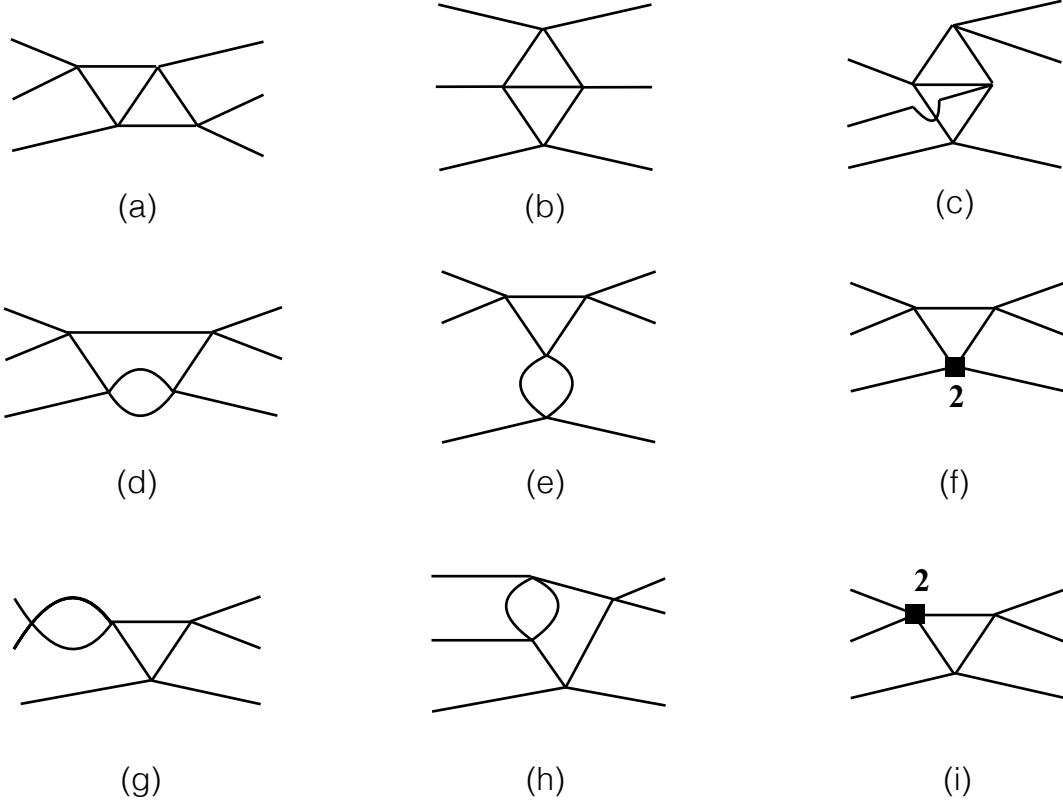


FIG. 5. A subset of Feynman diagrams contributing to $\partial_\tau C_{3,\text{thr}}^{(4)}(0)$ and $\mathcal{M}_{3,\text{thr}}$. Solid squares are vertex counterterms, with the number indicating the power of λ . External particles have zero three-momentum. Diagrams related by vertical or horizontal reflection are not shown.

1. Double triangle diagram: Fig. 5(a)

This is the first example of a class of diagrams arising first at fourth order, which involve a double triangle or diamond. Its IR behavior arises from a process in which there are three $2 \rightarrow 2$ scatterings, with the spectator particle alternating. As shown in Ref. [8], this leads to a logarithmic IR divergence in the corresponding threshold amplitude, requiring the subtraction of the fourth-order term Ξ_2 .

If one of the loop momenta vanishes, the result is

$$\partial_\tau C_{3,\text{thr,conn}}^{(4)} \supset \frac{3}{28m^5 L^{12}} \sum_{\vec{p} \neq 0} \frac{-2 + \mathcal{O}(p^2)}{p^6} \Rightarrow a_3^{(4)} \supset 32\mathcal{K}, \quad (77)$$

where I have used Eq. (A4) to obtain the second result.

The result if both loop momenta are nonzero is

$$\partial_\tau C_{3,\text{thr,conn}}^{(4)} \supset \frac{1}{48m^3 L^{12}} \sum_{\vec{p} \neq 0} \sum_{\vec{q} \neq 0} \frac{9}{16} \frac{g(\vec{p}, \vec{q})}{p^2 q^2 (W_{pq}^2 - 9m^2)}, \quad (78)$$

where $W_{pq} = \omega_p + \omega_q + \omega_{pq}$, $\omega_{pq}^2 = m^2 + (\vec{p} + \vec{q})^2$, and $g(\vec{p}, \vec{q})$ is a nonsingular function that I do not reproduce, except to note that $g(0, 0) = 3/m^2$. The logarithmic IR divergence can be seen by noting that, for small momenta,

$$W_{pq}^2 - 9m^2 = 6(p^2 + q^2 + \vec{p} \cdot \vec{q}) + \dots \quad (79)$$

As explained in the introduction to this section, the summand in Eq. (78) is the integrand of the contribution of the double-triangle diagram to \mathcal{M}_3 at threshold. The prescription of Ref. [8] to remove the IR divergences in this case is to subtract the quantity

$$\frac{1}{\lambda^4} \Xi_2(\vec{p}, \vec{q}) = \frac{9}{16m^2} \frac{H(\vec{p})^2 H(\vec{q})^2}{p^2 q^2 [p^2 + q^2 + (\vec{p} + \vec{q})^2]}, \quad (80)$$

where $H(\vec{p})$ is a UV regulator whose detailed form will not matter here other than the property $H(0) = 1$. After subtraction the result can be integrated and defines the contribution of this diagram to the threshold amplitude, which I label $\mathcal{M}_{3,\text{thr}}^{\text{DT}}$. Thus I proceed by adding and subtract the Ξ_2 term, leading to

$$\partial_\tau C_{3,\text{thr,conn}}^{(4)} \supset \frac{1}{48m^3 L^{12}} \sum_{\vec{p} \neq 0} \sum_{\vec{q} \neq 0} \left[\frac{9}{16} \frac{g(\vec{p}, \vec{q})}{p^2 q^2 (W_{pq}^2 - 9m^2)} - \frac{\Xi_2(\vec{p}, \vec{q})}{\lambda^4} \right] + \frac{1}{48m^3 L^{12}} \sum_{\vec{p} \neq 0} \sum_{\vec{q} \neq 0} \frac{\Xi_2(\vec{p}, \vec{q})}{\lambda^4} \quad (81)$$

$$= \frac{1}{48m^3 L^6} \int_{p,q} \left[\frac{9}{16} \frac{g(\vec{p}, \vec{q})}{p^2 q^2 (W_{pq}^2 - 9m^2)} - \frac{\Xi_2(\vec{p}, \vec{q})}{\lambda^4} \right] + \frac{1}{48m^3 L^{12}} \sum_{\vec{p} \neq 0} \sum_{\vec{q} \neq 0} \frac{\Xi_2(\vec{p}, \vec{q})}{\lambda^4} \quad (82)$$

$$= \frac{\mathcal{M}_{3,\text{thr}}^{(4,\text{DT})}}{48m^3 L^6} + \frac{3}{2^{18} \pi^6 m^5 L^6} \left(\frac{64\pi^4}{3} \log N_{\text{cut}} - \mathcal{C}_5 \right). \quad (83)$$

In the second line, the sum of the IR regulated difference has been replaced by an integral, which is valid up to a $1/L^7$ contribution arising from the difference between the sum and integral of an integrand with a $1/p^2$ divergence. To obtain the final form, the expression for the sum over Ξ_2 given in Eqs. (C18) and (C19) of Ref. [8] has been used.

2. Diver diagram: Fig. 5(d)

This diagram is combined with the A_{2s} part of the counterterm diagram Fig. 5(f). This turns out to be the most involved calculation from Fig. 5. I denote the momentum in the outer loop by p , while that in the diver's head loop by q .

If $\vec{p} = 0$, the IR divergence is sufficient to lead to a contribution at the desired order, specifically

$$\partial_\tau C_{3,\text{thr,conn}}^{(4)} \supset \frac{3}{2^{10} m^5 L^6} \frac{1}{L^6} \sum_{\vec{q} \neq 0} \frac{1 + \mathcal{O}(q^2)}{q^6} \Rightarrow a_3^{(4)} \supset -4\mathcal{K}. \quad (84)$$

If $\vec{p} \neq 0$, Fig. 5(d) alone gives

$$\partial_\tau C_{3,\text{thr,conn}}^{(4)} \supset \frac{3}{2^{11} m^3 L^{12}} \sum_{\vec{p} \neq 0} \sum_{\vec{q}} \frac{1}{\omega_p^3 \omega_q} \frac{g^D(\vec{p}, \vec{q})}{p^4 (W_{pq}^2 - 9m^2)}, \quad (85)$$

where g^D is a complicated function that is finite when p and/or q vanish. Thus the summand does not diverge when $\vec{q} = 0$, allowing the sum over \vec{q} to include this point. The sum over \vec{q} is UV divergent, but this is canceled by the counterterm contribution, which is

$$\partial_\tau C_{3,\text{thr,conn}}^{(4)} \supset -\frac{3A_{2s}}{2^8 m^3 L^9} \sum_{\vec{p} \neq 0} \frac{3\omega_p^2 - m^2}{\omega_p^3 p^4}. \quad (86)$$

Combining, I find

$$\partial_\tau C_{3,\text{thr,conn}}^{(4)} \supset \frac{3}{2^{11} m^3 L^6} (S_1 + S_2), \quad (87)$$

$$S_1 = \frac{1}{L^3} \sum_{\vec{p} \neq 0} \frac{f^D(p)}{\omega_p^3 p^4}, \quad (88)$$

$$f^D(p) = \int_q \frac{1}{\omega_q q^2} \left[q^2 \frac{g^D(\vec{p}, \vec{q})}{(W_{pq}^2 - 9m^2)} - (3\omega_p^2 - m^2) \right], \quad (89)$$

$$S_2 = \frac{1}{L^3} \sum_{\vec{p} \neq 0} \frac{1}{\omega_p^3 p^4} \left[\frac{1}{L^3} \sum_{\vec{q}} - \int_q \right] \frac{g^D(\vec{p}, \vec{q})}{\omega_q (W_{pq}^2 - 9m^2)}. \quad (90)$$

Consider first S_1 . Its IR behavior is determined by the form of $f^D(p)$ near $p = 0$. Using the explicit form of g^D I find that $f^D(0) = 0$. To next pull out the leading IR behavior of the integrand using Eq. (79):

$$f^D(p) = \tilde{f}^D(p) + 2mI^D(p), \quad (91)$$

$$\tilde{f}^D(p) = \int_q \left[\frac{g^D(\omega_p, \omega_q, \omega_{pq})}{\omega_q (W^2 - 9m^2)} - \frac{2m}{p^2 + q^2 + \vec{p} \cdot \vec{q}} - \frac{3\omega_p^2 - m^2 - 2m\omega_q}{\omega_q q^2} \right], \quad (92)$$

$$I^D(p) = \int_q \left[\frac{1}{p^2 + q^2 + \vec{p} \cdot \vec{q}} - \frac{1}{q^2} \right], \quad (93)$$

The key property of the residue function is that $f^D(p) \propto p^2$ near $p = 0$. The integral I^D is well defined as long as one does the angular integral first, and gives

$$I^D(p) = -\frac{\sqrt{3}p}{8\pi}. \quad (94)$$

This shows that $f^D(p)$ is a function of p and not p^2 . Combining these results yields the S_1 contribution to $\partial_\tau C_{3,\text{thr,conn}}^{(4)}$:

$$\partial_\tau C_{3,\text{thr,conn}}^{(4)} \supset \frac{1}{48m^3 L^6} \frac{9}{2^7 L^3} \sum_{\vec{p} \neq 0} \left[-\frac{\sqrt{3}m}{4\pi\omega_p^3 p^3} + \frac{\tilde{f}^D(p)}{\omega_p^3 p^4} \right]. \quad (95)$$

The next step is to express this result in terms of the contribution of the diver diagram to $\mathcal{M}_{3,\text{thr}}$, which I denote $\mathcal{M}_{3,\text{thr}}^D$, and determine the remainder. Using the general result described in the introduction to this subsection, it follows from Eq. (95) that the contribution of the diver diagram to the amplitude at threshold is

$$\mathcal{M}_3^{(4,D)} = \frac{9}{2^7} \int_p \left[-\frac{\sqrt{3}m}{4\pi\omega_p^3 p^3} + \frac{\tilde{f}^D(p)}{\omega_p^3 p^4} \right]. \quad (96)$$

This is IR divergent, and to obtain $\mathcal{M}_{3,\text{thr}}^{(4,D)}$ one must subtract from this integral of the λ^4 part of Ξ_1 . The full expression for Ξ_1 is [see Eqs. (191)-(121) of Ref. [8]]

$$\Xi_1(p) = -\frac{9\lambda^3}{8m} \left[\frac{H(\vec{p})^2}{p^4} + \frac{\lambda}{32\pi m} \frac{\sqrt{3} H(\vec{p})^3}{2 p^3} \right], \quad (97)$$

and I need here only the second term. Thus I find

$$\mathcal{M}_{3,\text{thr}}^{(4,D)} = \frac{9}{2^7} \int_p \left[-\frac{\sqrt{3}m}{4\pi\omega_p^3 p^3} + \frac{\sqrt{3}H(\vec{p})^3}{4\pi m^2 p^3} + \frac{\tilde{f}^D(p)}{\omega_p^3 p^4} \right], \quad (98)$$

which indeed is IR (as well as UV) convergent. This allows the result (95) to be rewritten as

$$\partial_\tau C_{3,\text{thr,conn}}^{(4)} \supset \frac{\mathcal{M}_{3,\text{thr}}^{(4,D)}}{48m^3 L^6} - \frac{3}{2^{11}m^3 L^9} \sum_{\vec{p} \neq 0} \frac{\sqrt{3}H(\vec{p})^3}{4\pi m^2 p^3} \quad (99)$$

$$= \frac{\mathcal{M}_{3,\text{thr}}^{(4,D)}}{48m^3 L^6} - \frac{1}{48m^3 L^6} \frac{\chi_{1,B}}{\lambda^4} \quad (100)$$

$$= \frac{\mathcal{M}_{3,\text{thr}}^{(4,D)}}{48m^3 L^6} - \frac{3}{2^{18}\pi^6 m^5 L^6} \left(16\pi^3 \sqrt{3} \log N_{\text{cut}} + \mathcal{C}_4 \right). \quad (101)$$

In the second step I use the definition of $\chi_{1,B}$ given in Eq. (C13) of Ref. [8], and in the last step I use the evaluation of $\chi_{1,B}$ presented in Eq. (C15) of that work.

Now I turn to S_2 . Naively, it appears that the sum-integral difference appearing in Eq. (90) is exponentially suppressed, because there are no singularities in the region of integration over \vec{q} when $\vec{p} \neq 0$ (since $W_{pq} > 3m$). However the singularities are nearby, and the ‘‘suppression’’ is by $\exp(-pL) \sim \mathcal{O}(L^0)$. It follows that this term must be kept. Fortunately, it turns out that it can be related analytically to the \mathcal{C}_F contribution to $\Delta_{32}^{(4)}$ in Eq. (23).

To do so I rewrite S_2 by setting $W_{pq} \rightarrow 3m$ everywhere except for the $1/(W_{pq} - 3m)$ pole. This leads only to corrections suppressed by $\exp(-mL)$. Using the result

$$\left. \frac{g^D(\omega_p, \omega_q, \omega_{pq})}{W_{pq} + 3m} \right|_{W_{pq}=3m} = \frac{\omega_p^2(m + \omega_p)^2}{2m^2}, \quad (102)$$

I find

$$S_2 = -\frac{1}{L^3} \sum_{\vec{p} \neq 0} \frac{1}{p^4} \frac{(m + \omega_p)^2}{2m^2} \left[\frac{1}{L^3} \sum_{\vec{q}} - \int_q \right] \frac{1}{\omega_p \omega_q \omega_{pq} (3m - W_{pq})}. \quad (103)$$

Observing that the sum over \vec{p} is dominated by $p \sim 1/L$, and dropping higher order corrections in $1/L$, this can be rewritten as

$$S_2 = -\frac{1}{L^3} \sum_{\vec{p} \neq 0} \frac{2}{p^4} \left[\frac{1}{L^3} \sum_{\vec{q}} - \int_q \right] \frac{1}{\omega_p \omega_q \omega_{pq} (3m - W_{pq})} = -\frac{2^7}{9} \frac{\chi_F}{\lambda^4}. \quad (104)$$

Here χ_F is a quantity introduced in Ref.[8], which evaluates to

$$\chi_F = \lambda^4 \frac{9}{2^{14}\pi^6 m^2} \mathcal{C}_F. \quad (105)$$

Combining these results with Eq. (87) I find the contribution of the S_2 term to be

$$\partial_\tau C_{3,\text{thr,conn}}^{(4)} \supset -\frac{3}{2^{18}\pi^6 m^5 L^6} \mathcal{C}_F. \quad (106)$$

3. Figure 5(e)

This diagram is combined with the $A_{2t} + A_{2u}$ contribution from Fig. 5(f). I denote the momentum in the bull’s head loop by p and the other loop momentum by q . The sum over \vec{q} can be replaced by an integral since the summand is IR finite. For any nonzero choice of \vec{p} , the factorization of the two loops then implies that there is an exact cancellation between Figs. 5(e) and (f). For $\vec{p} = 0$ the absence of an IR divergence in \vec{q} implies that the contribution is of $\mathcal{O}(L^{-9})$.

Thus these diagrams make no contribution to $\partial_\tau C_{3,\text{thr,conn}}^{(4)}$.

They also make no contribution to $\mathcal{M}_{3,\text{thr}}$. To understand this first note that both the relevant IR subtraction terms in the definition of $\mathcal{M}_{3,\text{thr}}$, Eq. (76), namely Ξ_1 and Ξ_2 , have already been used for the earlier diagrams. Thus the contribution of Fig. 5(e) together with the counterterm must be IR finite by itself. This is a somewhat subtle issue since the bull’s head loop alone has a nonintegrable $1/p^4$ dependence in the IR [9]. To understand this issue requires using the IR regularization defined in Ref. [8]: external momenta are set to zero, and an IR cutoff is applied to the loop momentum, $p \geq \delta$. The result should then be IR finite when $\delta \rightarrow 0$. The point is that, since the two loops factorize, the cancelation with the counterterm is exact for any nonzero \vec{p} , and so the contribution to $\mathcal{M}_{3,\text{thr}}$ vanishes for all nonzero δ and thus also in the limit $\delta \rightarrow 0$.

4. Figure 5(g)

Figure. 5(g) combines with the A_{2s} part of Fig. 5(i), together with horizontal reflections. Viewed as a contribution to $\mathcal{M}_{3,\text{thr}}$, the argument given for the previous diagram continues to hold: there is an exact cancellation between the s-channel loop and its counterterm. This is not the case, however, when the diagram is evaluated as a contribution to $\partial_\tau C_{3,\text{thr}}^{(4)}(0)$. This is because the s-channel loop momentum is summed in Fig. 5(g) but integrated (in A_{2s}) in Fig. 5(i). The sum-integral difference leads to a finite-volume residue that, combined with the IR divergence from the bull's head diagram, leads to a $1/L^6$ correction.

There are three contributions of this type. The first occurs when both loop momenta are nonzero:

$$\partial_\tau C_{3,\text{thr,conn}}^{(4)} \supset \frac{3}{2^9 m^5 L^6} \frac{1}{L^3} \sum_{\vec{p} \neq 0} \frac{m^4}{\omega_{\vec{p}}^3 p^4} \left[\frac{1}{L^3} \sum_{\vec{q} \neq 0} - \int_q \right] \frac{1 + 3\vec{p}^2/(2m^2)}{\omega_q q^2} \quad (107)$$

$$= \frac{3}{2^{18} m^5 L^6} (8\mathcal{I}\mathcal{J}). \quad (108)$$

The second arises when the s-channel loop momentum vanishes:

$$\partial_\tau C_{3,\text{thr,conn}}^{(4)} \supset \frac{3}{2^9 m^5 L^6} \frac{1}{L^6} \sum_{\vec{p} \neq 0} \frac{-2 + \mathcal{O}(p^2)}{p^6} = \frac{3}{2^{18} \pi^6 m^5 L^6} (-16\mathcal{K}), \quad (109)$$

The final contribution occurs when the bull's head loop momentum vanishes:

$$\partial_\tau C_{3,\text{thr,conn}}^{(4)} \supset \frac{3}{2^9 m^5 L^6} \frac{1}{L^6} \sum_{\vec{q} \neq 0} \frac{1 + \mathcal{O}(q^2)}{q^6} = \frac{3}{2^{18} \pi^6 m^5 L^6} (8\mathcal{K}). \quad (110)$$

In total, this diagram gives

$$a_2^{(4)} \supset -8\mathcal{I}\mathcal{J} + 8\mathcal{K}. \quad (111)$$

5. Figure 5(h)

The final diagram of this class is Fig. 5(h), which combines with the $A_{2t} + A_{2u}$ part of Fig. 5(i). Here the argumentation is not so straightforward since the two loops do not factorize. Thus, while the UV divergence is canceled by the counterterm, there will be a finite residue. This residue vanishes, however, when the momentum in the bull's head loop itself vanishes. This in turn implies that the IR divergence in the bull's head loop is canceled. It then follows that the difference between the momentum sum and integral is exponentially suppressed, so that the contribution to $\partial_\tau C_{3,\text{thr}}^{(4)}(0)$ is simply of the standard form, Eq. (75).

6. Double fish diagram: Fig. 6(a)

I now turn to the two-loop radiative corrections to the three-particle tree diagram, starting with those involving two separate loops, shown in Fig. 6. The first diagram is that containing two s-channel fish, Fig. 6(a), which combines with the contributions to Fig. 6(d) and (f) in which the counterterms are A_{2s} .

If one momentum vanishes the result is

$$\partial_\tau C_{3,\text{thr,conn}}^{(4)} \supset 2 \times \frac{3}{2^{11} m^5 L^6} \frac{1}{L^6} \sum_{\vec{p} \neq 0} \frac{1 + \mathcal{O}(p^2)}{p^6} \Rightarrow a_2^{(4)} \supset -4\mathcal{K}, \quad (112)$$

where the initial factor of 2 arises because there are two choices of vanishing loop momentum.

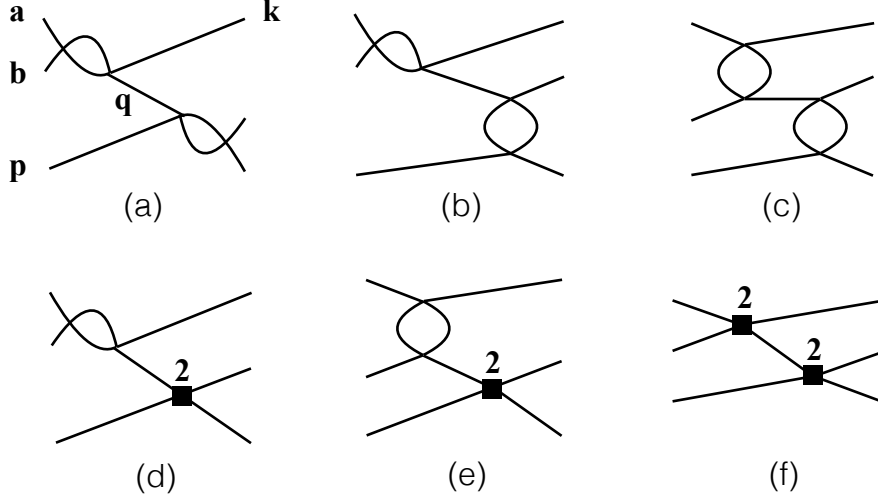


FIG. 6. Further diagrams contributing to $\partial_\tau C_{3,\text{thr,conn}}^{(4)}$ and $\mathcal{M}_{3,\text{thr}}$. Reflections are not shown.

If both momenta are nonvanishing then I find

$$\partial_\tau C_{3,\text{thr,conn}}^{(4)} \supset \frac{3}{2^{11} m^5 L^6} \left\{ \left[\frac{1}{L^3} \sum_{\vec{p} \neq 0} - \int_p \right] \left[\frac{1}{L^3} \sum_{\vec{q} \neq 0} - \int_q \right] \frac{1}{\omega_p p^2} \frac{1}{\omega_q q^2} \right. \\ \left. - \frac{1}{L^3} \sum_{\vec{p} \neq 0} \left[\frac{1}{L^3} \sum_{\vec{q} \neq 0} - \int_q \right] \frac{m^2}{\omega_p p^4} \frac{1}{\omega_q q^2} - \frac{1}{L^3} \sum_{\vec{q} \neq 0} \left[\frac{1}{L^3} \sum_{\vec{p} \neq 0} - \int_p \right] \frac{1}{\omega_p p^2} \frac{m^2}{\omega_q q^4} \right\} \quad (113)$$

$$\Rightarrow a_2^{(4)} \supset -4\mathcal{I}\mathcal{J}. \quad (114)$$

All contributions here involve at least one sum-integral difference, a result that arises due to the cancelation with counterterms. Thus there is no contribution to $\partial_\tau C_{3,\text{thr,conn}}^{(4)}$ of the standard form involving $\mathcal{M}_{3,\text{thr}}$, Eq. (75). This implies that, in order to be consistent with Eq. (23), the double-fish diagram, viewed as an infinite-volume scattering diagram, must give a vanishing contribution to $\mathcal{M}_{3,\text{thr}}^{(4)}$.

To see that this is indeed the case, I recall how the IR regulation and subtraction of Ref. [8] works for such a diagram. Since the diagram diverges at threshold (due to the intermediate propagator), one must insert momenta, then perform the subtraction (in this case of $I_{0,\delta}$), and then take the threshold limit. Using the labeling in Fig. 6(a), the momentum configuration chosen in Ref. [8] is that the spectator momenta vanish ($\vec{p} = \vec{k} = 0$), implying that the momentum flowing through the intermediate propagator also vanishes, $\vec{q} = \vec{P} - \vec{p} - \vec{k} = 0$, while the “nonspectator pair” have nonzero momenta, $\vec{a} = -\vec{b} \neq 0$. The CM energy flowing through the diagram is then

$$E = 3m + \frac{a^2}{m} + \mathcal{O}(a^4/m^3). \quad (115)$$

The intermediate propagator is

$$\Delta(q) = \frac{i}{q^2 - m^2 + i\epsilon} = \frac{i}{(E - m)(E - 3m + i\epsilon)}, \quad (116)$$

and the $i\epsilon$ can be dropped provided $a \neq 0$. The scattering amplitudes attached to both vertices are then partially off shell, since $q^2 \neq m^2$. I label them $\mathcal{M}_{2,\text{off}}^{(2,S)}$, with the superscript indicating 2 for second order and S for s-channel loop. According the definition in Ref. [8], this amplitude should be s-wave projected. However, this is automatically satisfied here, since the amplitude depends only on $s = 4(m^2 + a^2) \equiv s_a$ and not on the direction of \vec{a} . The result is

thus

$$i\mathcal{M}_3^{(u,u)} \supset i\mathcal{M}_{2,\text{off}}^{(2,S)}(s_a) \frac{i}{(E-m)(E-3m)} i\mathcal{M}_{2,\text{off}}^{(2,S)}(s_a). \quad (117)$$

The superscript (u,u) on \mathcal{M}_3 follows the notation of Ref. [8] and indicates that the amplitude is unsymmetrized.

In order to obtain a finite threshold amplitude, the appropriate part of $I_{0,s}$ must be subtracted. This is [8]

$$iI_0^{(u,u)} = i\mathcal{M}_{2,s}^{(2,S)}(s_a) iG_s^\infty i\mathcal{M}_{2,s}^{(2,S)}(s_a), \quad (118)$$

$$iG_s^\infty = \frac{i}{2m(E-3m+i\epsilon)}, \quad (119)$$

where again the $i\epsilon$ can be dropped. Here the subscript $2,s$ indicates that this is contribution to the two-particle s-wave scattering amplitude. Now I note that the s-channel loop amplitude is independent of the value of q^2 , so that, in fact, $\mathcal{M}_{2,\text{off}}^{(2,S)} = \mathcal{M}_{2,s}^{(2,S)}$. Thus the difference between Eqs. (117) and (118) can be simplified to

$$i\left(\mathcal{M}_3^{(u,u)} - I_0^{(u,u)}\right) = i\mathcal{M}_{2,s}^{(2,S)}(s_a) \frac{1}{2m(E-m)} \mathcal{M}_{2,s}^{(2,S)}(s_a) \xrightarrow{E \rightarrow 3m} i\mathcal{M}_{2,s}^{(2,S)}(4m^2) \frac{1}{(2m)^2} \mathcal{M}_{2,s}^{(2,S)}(4m^2) = 0. \quad (120)$$

In the last step I have taken the threshold limit by sending $a \rightarrow 0$, which is possible since the IR divergence has canceled. I find that the result vanishes in this limit because, by definition, all second and higher-order contributions to the scattering amplitude vanish at threshold. The final step is to symmetrize the result, which does not change the fact that the result vanishes. Thus the double-fish diagram does not contribute to $\mathcal{M}_{3,\text{thr}}^{(4)}$.

7. Fish and sinker diagram: Fig. 6(b)

This diagram combines with the $A_{2t} + A_{2u}$ part of Fig. 6(d), the A_{2s} part of Fig. 6(e), and the $(A_{2t} + A_{2u})A_{2s}$ part of Fig. 6(f), together with horizontal reflections. When evaluating the contribution to $\partial_\tau C_{3,\text{thr,conn}}^{(4)}$, the momentum integrals in the counterterms can be converted into sums at the order I work. I then find that the total summand vanishes identically, so that there is no contribution to $\partial_\tau C_{3,\text{thr,conn}}^{(4)}$. As for the double-fish diagram, this implies that, if Eq. (23) is to hold, then the fish and sinker diagram must give no contribution to $\mathcal{M}_{3,\text{thr}}^{(4)}$.

The argument that this is the case is more subtle than for the double-fish diagram, because the off-shell two-to-two amplitude appearing at the right-hand vertex in Fig. 6(b) now depends on q^2 . I label this amplitude $\mathcal{M}_{2,\text{off}}^{(2,T)}(s_a, t_a, u_a)$, with the superscript T indicating the t/u-channel loop. Because it is off shell it depends on all three Mandelstam variables, and thus on q^2 through the relation $s_a + t_a + u_a = 3m^2 + q^2$. For the kinematic configuration explained above the Mandelstam variables are $s_a = 4(m^2 + a^2)$ and $t_a = u_a = m(3m - E)$. Since these are independent of the direction of \vec{a} , the off-shell amplitude is pure s-wave so there is no need to apply the s-wave projection. The IR subtraction now takes the form (before symmetrization)

$$i\mathcal{M}_{2,\text{off}}^{(2,S)}(s_a) \frac{i}{(E-m)(E-3m)} i\mathcal{M}_{2,\text{off}}^{(2,T)}(s_a, t_a, u_a) - i\mathcal{M}_{2,s}^{(2,S)}(s_a) \frac{i}{2m(E-3m)} i\mathcal{M}_{2,s}^{(2,T)}(s_a), \quad (121)$$

where in the second term $\mathcal{M}_{2,s}^{(2,T)}$ is the contribution to the on-shell, s-wave, two-particle amplitude coming from the t/u-channel diagram. I stress that this is not the same as $\mathcal{M}_{2,\text{off}}^{(2,T)}$, although the difference vanishes at threshold since both quantities vanish there. The difference can be rewritten as

$$i\mathcal{M}_{2,s}^{(2,S)}(s_a) \frac{i}{2m(E-m)} i\mathcal{M}_{2,s}^{(2,T)}(s_a) + i\mathcal{M}_{2,s}^{(2,S)}(s_a) \frac{i}{2m(E-3m)} \left[i\mathcal{M}_{2,\text{off}}^{(2,T)}(s_a, t_a, u_a) - i\mathcal{M}_{2,s}^{(2,T)}(s_a) \right], \quad (122)$$

Both terms are finite when $E \rightarrow 3m$, but again the limiting value is zero because $\mathcal{M}_{2,s}^{(2,S)}$ vanishes at threshold.

8. Double-sinker diagram: Fig. 6(c)

This diagram combines with the contributions from Figs. 6(e) and (f) in which the counterterms are $A_{2t} + A_{2u}$. Here both loop sums can be converted to integrals, and the cancelation with the counterterms is exact. Thus there is no contribution to $\partial_\tau C_{3,\text{thr,conn}}^{(4)}$.

Because of this I expect no contribution from these diagrams also to $\mathcal{M}_{3,\text{thr}}^{(4)}$. Including the subtraction, the result for the unsymmetrized amplitude is

$$i\mathcal{M}_{2,\text{off}}^{(2,\text{T})}(s_a, t_a, u_a) \frac{i}{(E-m)(E-3m)} i\mathcal{M}_{2,\text{off}}^{(2,\text{T})}(s_a, t_a, u_a) - i\mathcal{M}_{2,s}^{(2,\text{T})}(s_a) \frac{i}{2m(E-3m)} i\mathcal{M}_{2,s}^{(2,\text{T})}(s_a). \quad (123)$$

Using the facts that $\mathcal{M}_{2,\text{off}}^{(2,\text{T})}(s_a, t_a, u_a) - \mathcal{M}_{2,s}^{(2,\text{T})}(s_a) \propto (E-3m)$ [with the explicit form of this difference given in Eq. (58) of Ref. [8]] and $\mathcal{M}_{2,s}^{(2,\text{T})}(4m^2) = 0$, the difference (123) can be shown to vanish when $E \rightarrow 3m$.

9. *SS single-fish diagram: Fig. 7(a)*

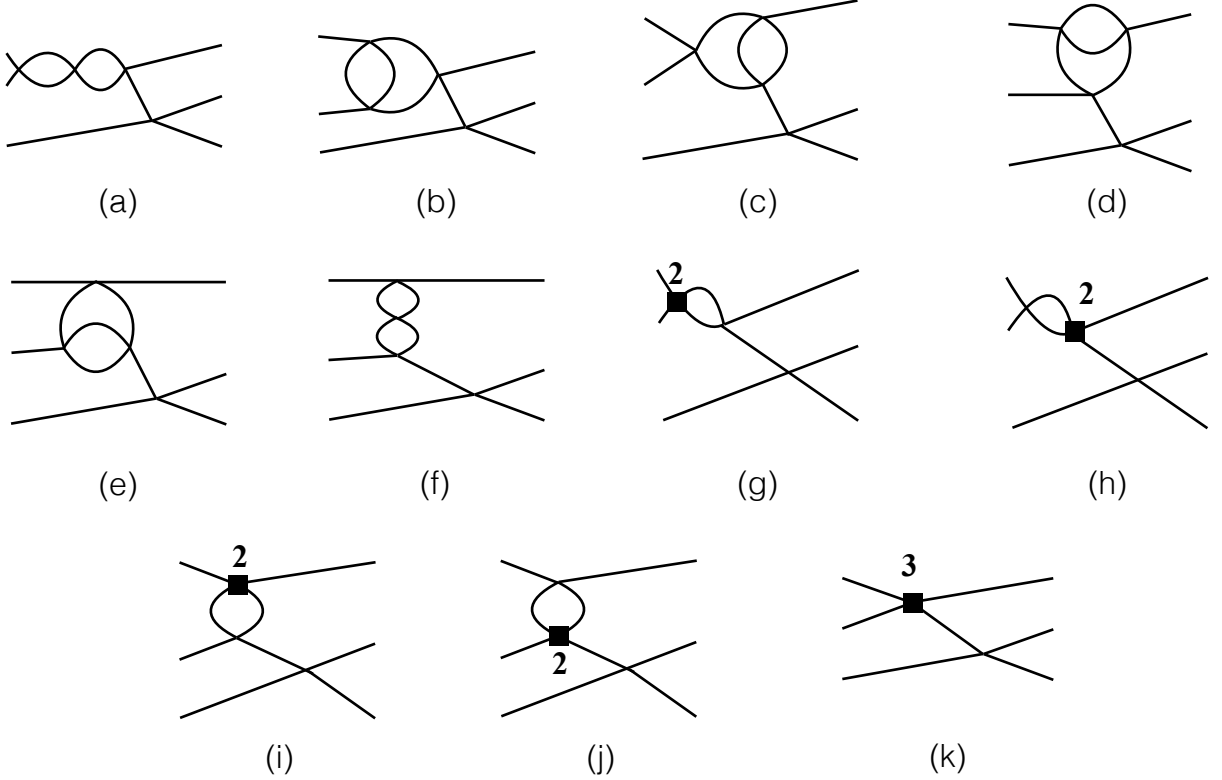


FIG. 7. Further diagrams contributing to $\partial_r C_{3,\text{thr,conn}}^{(4)}$ and $\mathcal{M}_{3,\text{thr}}$. Reflections are not shown.

I now move to radiative corrections to the three-particle tree diagram that involve a single two-loop correction. These diagrams are shown in Fig. 7, and I begin with that involving a “fish” with two s-channel loops, Fig. 7(a), which combines with the A_{2s} parts of Figs. 7(g) and (h) and the A_{3ss} part of Fig. 7(k), along with their horizontal reflections.

If both momenta are nonzero, the result has the same form as that for the double-fish diagram, Eq. (113), except for an overall additional factor of 2 because of the reflected diagram. Similarly there are contributions when one of the loop momenta vanishes that are twice those from the double-fish diagram. Thus in total I find

$$a_2^{(4)} \supset 8\mathcal{I}\mathcal{J} - 8\mathcal{K}. \quad (124)$$

Turning now to the contribution to $\mathcal{M}_{3,\text{thr}}^{(4)}$, the subtracted amplitude takes the form

$$i\mathcal{M}_{2,\text{off}}^{(3,\text{SS})}(s_a) \frac{i}{(E-m)(E-3m)} (-i) - i\mathcal{M}_{2,s}^{(3,\text{SS})}(s_a) \frac{i}{2m(E-3m)} (-i), \quad (125)$$

where the superscript indicates the third-order contribution involving two s-channel loops. As above, the s-channel loops give a result that does not depend on the off-shellness, q^2 , so $\mathcal{M}_{2,\text{off}}^{(3,\text{SS})} = \mathcal{M}_{2,s}^{(3,\text{SS})}$. Thus the difference (125) can be written as

$$i\mathcal{M}_{2,s}^{(3,\text{SS})}(s_a) \frac{1}{m(m-E)} \xrightarrow{E \rightarrow 3m} -i\mathcal{M}_{2,s}^{(3,\text{SS})}(4m^2) \frac{1}{2m^2}, \quad (126)$$

which vanishes because $\mathcal{M}_{2,s}^{(3,\text{SS})}(4m^2) = 0$.

10. TS fish diagram: Fig. 7(b)

This diagram combines with the $A_{2t} + A_{2u}$ part of Fig. 7(g), and the A_{3st} part of Fig. 7(k), plus reflections.

In this case the contribution to $\partial_\tau C_{3,\text{thr}}^{(4)}(0)$ does not vanish because the cancelation with the counterterms is not exact. The result can be written (after converting counterterm integrals into sums) as

$$\partial_\tau C_{3,\text{thr,conn}}^{(4)} \supset \frac{3}{2^9 m^5 L^6} \frac{1}{L^6} \sum_{\vec{p}, \vec{q}} f^{\text{TS}}(\vec{p}, \vec{q}). \quad (127)$$

The sum is convergent in the IR and UV and thus can be replaced by an integral at the order I work. The result of the numerical integration is

$$\partial_\tau C_{3,\text{thr,conn}}^{(4)} \supset \frac{3}{2^9 m^5 L^6} \frac{I^{\text{TSf}}}{8\pi^4}, \quad I^{\text{TSf}} = I^{\text{STS0}}. \quad (128)$$

The agreement with I^{STS0} is to the accuracy of the numerical evaluation.

Turning now to the contribution to $\mathcal{M}_{3,\text{thr}}$, I again find it vanishes. The argument is as for the SS fish diagram, and relies on the result that $\mathcal{M}_{2,\text{off}}^{(3,TS)}$ depends only on s_a (and not on q^2), implying that it equals $\mathcal{M}_{2,s}^{(3,TS)}$, and also that $\mathcal{M}_{2,s}^{(3,TS)}(4m^2) = 0$.

11. ST fish diagram: Fig 7(c)

The ST fish diagram combines with the $A_{2t} + A_{2u}$ part of Fig. 7(h) and the A_{3st} part of Fig. 7(k), plus reflections.

As for the TS diagram the contribution to $\partial_\tau C_{3,\text{thr}}^{(4)}(0)$ involves an IR and UV convergent sum that can be converted to an integral. Numerical evaluation leads to

$$\partial_\tau C_{3,\text{thr,conn}}^{(4)} \supset \frac{3}{2^9 m^5 L^6} \frac{I^{\text{STf}}}{8\pi^4}, \quad I^{\text{STf}} = 0.355066. \quad (129)$$

The ST fish diagram also gives a nonvanishing contribution to $\mathcal{M}_{3,\text{thr}}^{(4)}$. This can be written as

$$i\mathcal{M}_{3,\text{thr}}^{(4,\text{STf})} = \lim_{E \rightarrow 3m} 2\mathcal{S} \left\{ i \left[\mathcal{M}_{2,\text{off}}^{(3,ST)}(s_a, t_a, u_a) - \mathcal{M}_{2,s}^{(3,ST)}(s_a) \right] \frac{i}{q^2 - m^2} (-i) \right\}, \quad (130)$$

where the overall factor of 2 arises from the reflection, and \mathcal{S} indicates symmetrization over the choice of initial and final state spectator particle (which in the end simply leads to a factor of 9). The superscripts indicate the third-order ST scattering diagram contained in Fig. 7(c), and I have simplified using the result that $\mathcal{M}_{2,s}^{(3,ST)}(4m^2) = 0$. The difference between off- and on-shell amplitudes is proportional to $q^2 - m^2$ and thus leads to a finite result in the limit.

To determine this result requires calculating the off-shell two-loop amplitude near threshold. This is closely related to the calculation of the two-loop contribution to the scattering length presented in Appendix C, and thus I present the details of the off-shell calculation in App. C 2 a. The result is that

$$\mathcal{M}_{3,\text{thr}}^{(4,\text{STf})} = 9 \frac{1}{m^2 (4\pi)^4} I^{\text{STM}}, \quad I^{\text{STM}} = 0.214978. \quad (131)$$

Combining this with the result (129) leads to the total contribution from this diagram

$$\partial_\tau C_{3,\text{thr,conn}}^{(4)} \supset \frac{\mathcal{M}_{3,\text{thr}}^{(4,\text{STf})}}{48m^3 L^6} + \frac{3(I^{\text{STf}} - I^{\text{STM}})}{2^{12} \pi^4 m^5 L^6}. \quad (132)$$

12. *TT fish diagram: Fig. 7(f)*

This diagram combines with the A_{2t} parts of Figs. 7(i) and (j), and the $A_{3tt} + A_{3uu}$ part of Fig. 7(k), together with reflections.

The contribution to $\partial_\tau C_{3,\text{thr}}^{(4)}(0)$ is simple enough to reproduce in full:

$$\partial_\tau C_{3,\text{thr,conn}}^{(4)} \supset \frac{3}{2^9 m^5 L^6} \frac{1}{L^6} \sum_{\bar{p}, \bar{q}} \frac{m^3}{4\omega_p^3(\omega_p + m)\omega_q^3(\omega_q + m)(\omega_p + \omega_q)} = \frac{3}{2^9 m^5 L^6} \frac{I^{\text{TT}}}{32\pi^4} + \mathcal{O}(L^{-7}). \quad (133)$$

The value of I^{TT} is given in Eq. (38).

There is also a potential contribution to $\mathcal{M}_{3,\text{thr}}^{(4)}$ that, before symmetrization, has the form

$$2i \left[\mathcal{M}_{2,\text{off}}^{(3,\text{TT})}(s_a, t_a, u_a) - \mathcal{M}_{2,s}^{(3,\text{TT})}(s_a) \right] \frac{i}{q^2 - m^2} (-i). \quad (134)$$

Since the two t-channel loops factorize, however, I can use the result from Ref. [9] that a single such loop gives a contribution proportional to $q^2 - m^2$. This implies that the contribution of two loops is proportional to $(q^2 - m^2)^2$, so that the overall result vanishes at threshold when $q^2 \rightarrow m^2$.

13. *SU fish diagram: Fig. 7(d)*

This diagram combines with the $A_{2s} + A_{2u}$ part of Fig. 7(i), and the $A_{3tu}/2$ part of Fig. 7(k), as well as the reflections of all diagrams.

The contribution to $\partial_\tau C_{3,\text{thr}}^{(4)}(0)$ is again a finite integral

$$\partial_\tau C_{3,\text{thr,conn}}^{(4)} \supset \frac{3}{2^8 m^5 L^6} \frac{I^{\text{SU}}}{16\pi^4}, \quad (135)$$

where I^{SU} is given in Eq. (39).

The contribution to $\mathcal{M}_{3,\text{thr}}^{(4)}$ is worked out in App. C 2 b, yielding

$$\mathcal{M}_{3,\text{thr}}^{(4,\text{SUf})} = 9 \frac{1}{m^2 (4\pi)^4} (-I^{\text{SUr}}), \quad I^{\text{SUr}} = -0.274156. \quad (136)$$

Thus in total the SU fish diagram gives

$$\partial_\tau C_{3,\text{thr,conn}}^{(4)} \supset \frac{\mathcal{M}_{3,\text{thr}}^{(4,\text{SUf})}}{48m^3 L^6} + \frac{3(I^{\text{SU}} + I^{\text{SUr}})}{2^{12} \pi^4 m^5 L^6}. \quad (137)$$

14. *US fish diagram: Fig. 7(e)*

This is the final diagram of this class, and combines with the $A_{2s} + A_{2u}$ part of Fig. 7(j) and the $A_{3tu}/2$ part of Fig. 7(k), as well as reflections.

The contribution to $\partial_\tau C_{3,\text{thr}}^{(4)}(0)$ is

$$\partial_\tau C_{3,\text{thr,conn}}^{(4)} \supset \frac{3}{2^8 m^5 L^6} \frac{I^{\text{USf}}}{16\pi^4}, \quad I^{\text{USf}} = -0.13788. \quad (138)$$

The contribution to $\mathcal{M}_{3,\text{thr}}^{(4)}$ is worked out in App. C 2 c, and leads to

$$\partial_\tau C_{3,\text{thr,conn}}^{(4)} \supset \frac{\mathcal{M}_{3,\text{thr}}^{(4,\text{USf})}}{48m^3 L^6} + \frac{3(I^{\text{US}} - I^{\text{USM}})}{2^{12} \pi^4 m^5 L^6}, \quad I^{\text{USM}} = 0.096623. \quad (139)$$

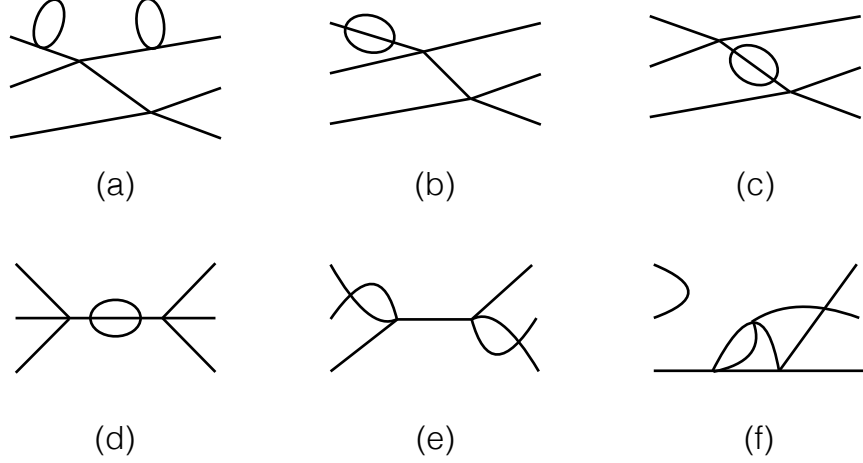


FIG. 8. Examples of Feynman diagrams contributing to $\partial_\tau C_{3,\text{thr,conn}}^{(4)}$ that do not lead to nonstandard finite-volume dependence. See text for further discussion.

C. Remaining diagrams

Finally, I discuss diagrams of various classes that turn out either not to contribute, or to contribute only results of the standard form, Eq. (75).

The first class are those with mass and wavefunction renormalization parts. Examples of their contributions to $\partial_\tau C_{3,\text{thr,conn}}^{(4)}$ are shown in Figs. 8 (a), (b) and (c). The arguments of Sec. III C can be used to show that, when combined with the corresponding counterterms these either cancel completely, which is the case for Fig. 8(a), or lead to contact terms, as is true for Figs. 8(b) and (c). These contact terms then either lead to contributions to the amplitudes $A_{j,k}$ of Eq. (6) alone, and not to $\Delta E_{3,\text{thr}}$, as is the case for Fig. 8(b), or lead to contributions to $\partial_\tau C_{3,\text{thr,conn}}^{(4)}$ of the standard form, Eq. (75), an example being Fig. 8(c).

There is one diagram, that of Fig. 8(d), requiring special treatment, because it has a physical cut through the renormalization part. This implies that there is a nonzero remainder when the momentum sums in this part are replaced by integrals. However, by explicit calculation I find that this remainder is subleading in $1/L$ because the IR divergence is rather weak. Thus this diagram also gives only the standard contribution of Eq. (75).

There are also many other diagrams that are one-particle reducible, e.g. Fig. 8(e). Although some of these diagrams, such as this example, have three-particle cuts, the resulting summands only have $1/p^2$ IR divergences and so sums can be converted to integrals at the order I work. Thus all such diagrams lead to contributions of the standard form, Eq. (75).

Finally, there are partially disconnected diagrams such as Fig. 8(f). As explained in Ref. [9], these amount to studying the three-particle threshold energy using, on one or both sides, an operator that creates a single particle, and can be dropped.

D. Summary

Combining the results from Eqs. (77), (83), (84), (101), (106), (111), (112), (114), (124), (128), (132), (137), and (139), and recalling the definitions Eqs. (27) and (28), leads to the following total contribution to $a_2^{(4)}$ from $\partial_\tau C_{3,\text{thr,conn}}^{(4)}$:

$$a_2^{(4)} \Big|_{\partial_\tau C_{3,\text{thr,conn}}^{(4)}} = -\frac{2^{14} m^2 \pi^6}{9} \mathcal{M}_{3,\text{thr}}^{(4)} + [4\mathcal{I}\mathcal{J} + 24\mathcal{K} + c_L \log(N_{\text{cut}}) + \mathcal{C}_4 + \mathcal{C}_5 + \mathcal{C}_F] - 2^6 \pi^2 (I^{\text{STS0}} + I^{\text{STf}} - I^{\text{STM}} + \frac{1}{4} I^{\text{TT}} + I^{\text{SU}} + I^{\text{SUR}} + I^{\text{US}} - I^{\text{USM}}). \quad (140)$$

Combining this result with those in Eqs. (71) and (74) gives the final result for $a_2^{(4)}$:

$$a_2^{(4)} = -\frac{2^{14}m^2\pi^6}{9}\mathcal{M}_{3,\text{thr}}^{(4)} + [2\mathcal{I}^2 - 8\mathcal{I}\mathcal{J} + 18\mathcal{K} + c_L \log(N_{\text{cut}}) + \mathcal{C}_4 + \mathcal{C}_5 + \mathcal{C}_F] + 2^6\pi^2\mathcal{R}, \quad (141)$$

$$\mathcal{R} = [I^{\text{SST}0} - I^{\text{STS}0}] + [I^{\text{STS}0} - I^{\text{STS}} - I^{\text{STf}} + I^{\text{STM}}] + [I^{\text{SU}} - 2I^{\text{SSU}} - I^{\text{SUR}}] + [2I^{\text{SU}} - I^{\text{US}} - 2I^{\text{SSU}} + I^{\text{USM}}]. \quad (142)$$

This result should be compared to that obtained from the general FV formalism, which, using Eq. (23), is given by the first two terms in Eq. (141). Thus agreement requires the residue \mathcal{R} to vanish. In fact, each of the four quantities in square brackets vanishes separately to within the numerical accuracy of integration (roughly five significant figures). This completes the desired check. The fact that cancelations occur in subsets of quantities indicates that the cancelations can be understood at a diagrammatic level.

V. CONCLUSIONS

The calculation presented here has confirmed the threshold expansion derived from the three-particle quantization condition of Refs. [3, 4]. It provides a further nontrivial test of the quantization condition as well as of the rather involved determination of the threshold expansion from the quantization condition [8].

Comparing the form of the predictions for $\Delta E_{2,\text{thr}}^{(4)}$ and $\Delta E_{3,\text{thr}}^{(4)}$, given in Eqs. (20) and (21) respectively, one sees that the latter contains additional “geometric” constants, \mathcal{C}_F , \mathcal{C}_4 , and \mathcal{C}_5 , as well as the $\mathcal{M}_{3,\text{thr}}$ term. The new constants arise from the need to subtract IR divergences from diagrams in which there is alternating pairwise two-particle scattering. The calculation presented here checks that these subtractions do the job for which they were designed. By working at fourth order all terms contributing to the IR subtraction have been tested.

As noted in Ref. [9], the result from the present relativistic calculation cannot be compared to those obtained using nonrelativistic QM both because relativistic effects enter at $\mathcal{O}(L^{-6})$ and because the nonrelativistic analogs of $\mathcal{M}_{3,\text{thr}}$ differ, in general, by finite amounts. Nevertheless, I observe that the coefficients of \mathcal{I}^3 , $\mathcal{I}\mathcal{J}$ and \mathcal{K} do agree with those of Ref. [11].

It will be interesting and useful to test other approaches to the three-particle quantization condition, such as that using a nonrelativistic, particle-dimer approach [6, 7], by confirming that they reproduce the three-particle threshold expansion.

ACKNOWLEDGMENTS

This work was supported in part by the United States Department of Energy grant No. DE-SC0011637. I thank Raúl Briceño, Max Hansen and John Spencer for discussions and comments.

Appendix A: Sum-integral differences

The following two results from Ref. [9] are used repeatedly in the main text

$$\left[\frac{1}{L^3} \sum_{\vec{p} \neq 0} - \int_p \right] \frac{f(p^2)}{p^2} = \frac{\mathcal{I}f(0)}{(2\pi)^2 L} - \frac{f'(0)}{L^3} \quad (\text{A1})$$

$$\frac{1}{L^3} \sum_{\vec{p} \neq 0} \frac{g(p^2)}{p^2} = \frac{L\mathcal{J}g(0)}{(2\pi)^4} + \int_p \frac{g(p^2) - g(0)}{p^4} + \mathcal{O}(L^{-1}). \quad (\text{A2})$$

\mathcal{I} and \mathcal{J} are numerical constants whose explicit values are not needed in this paper. The shorthand for integrals is defined by

$$\int_p \equiv \int \frac{d^3 p}{(2\pi)^3}. \quad (\text{A3})$$

I also need a third result,

$$\frac{1}{L^3} \sum_{\vec{p} \neq 0} \frac{h(p^2)}{p^6} = \frac{L^3 \mathcal{K}h(0)}{(2\pi)^6} + \mathcal{O}(L), \quad (\text{A4})$$

where $\mathcal{K} = \sum_{\vec{n}=0} 1/n^6$. This equation can be derived by writing $h(p^2) = h(0) + [h(p^2) - h(0)]$ and using Eq. (A2). These results hold if f , g and h are smooth functions that in particular are regular at $p^2 = 0$. All three equations have, in addition to the power-law corrections shown, exponentially suppressed corrections of the form $e^{-\sqrt{\bar{m}^2}L}$. The scale \bar{m}^2 depends on the form of $f(p^2)$, but is no larger than the position of the nearest singularity of f in the complex p^2 plane. For the functions I encounter this scale is usually given by the scalar mass, $\bar{m} \sim m$. The equations also assume that the sums and integrals have been regularized in the UV, if needed, although the form of the L -dependent terms does not depend on the details of the regularization.

Appendix B: Counterterm for the coupling constant

The counterterm for the coupling constant has the expansion¹⁴

$$\delta Z_\lambda = \lambda^2 A_2 + \lambda^3 A_3 + \lambda^4 A_4 + \dots, \quad (\text{B1})$$

A_2 is identical to the quantity of the same name used in Ref. [9]:

$$A_2 = A_{2s} + A_{2t} + A_{2u}, \quad (\text{B2})$$

$$A_{2s} = \int_p^\Lambda \frac{1}{8\omega_p \bar{p}^2}, \quad A_{2t} = A_{2u} = \int_p^\Lambda \frac{1}{8\omega_p^3}. \quad (\text{B3})$$

The superscript Λ indicates the necessity of UV regulation. For most of our calculations the form of the regulator can be left implicit, since in the end the integrals to be evaluated are UV convergent. However, when calculating the two-loop \mathbf{K} matrix the explicit form of the counterterms are needed. Using dimensional regularization, these are

$$A_{2t} = A_{2u} = \int \frac{d^{d-1}q}{(2\pi)^{d-1}} \frac{1}{8\omega_q^3} = \frac{\Gamma(2-d/2)}{(4\pi)^{d/2}} \frac{1}{2}, \quad (\text{B4})$$

$$A_{2s} = \int \frac{d^{d-1}q}{(2\pi)^{d-1}} \frac{1}{8q^2 \omega_q} = \frac{\Gamma(2-d/2)}{(4\pi)^{d/2}} \frac{1}{2} \frac{1}{d-3}, \quad (\text{B5})$$

where d is the number of space-time dimensions. I stress that these are the same counterterms as obtained by doing the d -dimensional momentum integrals directly, rather than the hybrid approach time/3-momentum approach used here.

¹⁴ The definition of A_3 used here differs from that of Ref. [9].

The calculations described in the main text also require the explicit form of A_3 . This is obtained by calculating the scattering amplitude at two loop order, including all counterterm contributions, and setting its value at threshold to zero. A convenient way of obtaining the integrand of the scattering amplitude is simply to calculate the diagrams contributing to $\partial_\tau C_{2,\text{thr}}^{(3)}$, using the methods described in Sec. II, and pick out the coefficient multiplying $1/(8m^2 L^3)$. The four two-loop diagrams are those in Fig. 1 (d), (e), (f) and (g), which I label respectively as SS, TT, SU and ST diagrams. These are combined with the counterterm diagrams in the same way as in the calculation of $\partial_\tau C_{2,\text{thr}}^{(3)}(0)$ in Sec. III. The corresponding two-loop counterterms are given by:

$$A_3 = A_{3ss} + A_{3tt} + A_{3su} + A_{3st}, \quad (\text{B6})$$

$$A_{3ss} = A_{2s}^2, \quad (\text{B7})$$

$$A_{3tt} = 2A_{2t}^2, \quad (\text{B8})$$

$$A_{3su} = \iint_{p,q}^\Lambda \left\{ 4A_{2t}(A_{2s} + A_{2u}) - \left[\frac{W_{pq}^3 + W_{pq}^2 \omega_p - W_{pq} m^2 + \omega_{pq} m^2}{4\omega_p^3 \omega_{pq} \omega_q (W_{pq}^2 - m^2)^2} \right] \right\}, \quad (\text{B9})$$

$$A_{3st} = \iint_{p,q}^\Lambda \frac{1}{32\omega_p^3 \omega_q q^2} \left[1 - \frac{2\omega_p^2 (W_{pq} + \omega_q)}{\omega_{pq} (W_{pq}^2 - m^2)} \right], \quad (\text{B10})$$

where $W_{pq} = \omega_p + \omega_{pq} + \omega_q$.

The calculations of Sec. IIIB also require parts of the counterterm A_4 , specifically those needed for Figs. 2(f)-(k). These are given by enforcing the renormalization condition, which implies that the coefficient of $1/L^3$ in the contribution to $\partial_\tau C_{2,\text{thr}}^{(4)}(0)$ of a given three-loop diagram, together with the counterterm diagrams, must vanish. The contributions to A_4 are thus easily determined in the course of the calculation. In general their form is long and uninformative, and I do not quote the results here.

Appendix C: Two-loop K matrix and related quantities

In this appendix I calculate the derivative of the s-wave K matrix at threshold, $\mathcal{K}'_{2,s,\text{thr}}$, defined in Eq. (18), at cubic order in λ . This is needed in order to check that the perturbative result obtained here, Eq. (65), agrees with the prediction from the quantization condition, Eq. (20). In addition I determine the partially off shell K matrix needed in order to define $\mathcal{M}_{3,\text{thr}}^{(4)}$, itself needed to test the result Eq. (23). These calculations are done in infinite volume using standard momentum-space methods for Feynman diagrams, and I only provide a sketch of the details.

1. Calculation of $\mathcal{K}'_{2,s,\text{thr}}^{(3)}$

I focus first on the on shell K matrix, which is a real, analytic function of q^2 , with q the momentum of each particle in the CM frame. It is most straightforward to use Feynman rules with the $i\epsilon$ prescription to determine the s-wave scattering amplitude $\mathcal{M}_{2,s}$, and then obtain $\mathcal{K}_{2,s}$ using the general relation¹⁵

$$\mathcal{K}_{2,s}(q^2) = \mathcal{M}_{2,s}(q) - \mathcal{M}_{2,s}(q) \frac{iq}{16\pi E} \mathcal{M}_{2,s}(q) + \mathcal{M}_{2,s}(q) \frac{iq}{16\pi E} \mathcal{M}_{2,s}(q) \frac{iq}{16\pi E} \mathcal{M}_{2,s}(q) + \mathcal{O}(\lambda^4). \quad (\text{C1})$$

Here E is the total CM energy. Expanding $\mathcal{K}_{2,s}$ and $\mathcal{M}_{2,s}$ in powers of λ , e.g. $\mathcal{K}_{2,s} = \sum_{n=1}^\infty \lambda^n \mathcal{K}_{2,s}^{(n)}$, and noting that there is no q dependence at leading order, I have $\mathcal{M}_{2,s}^{(1)} = \mathcal{K}_{2,s}^{(1)} = -\lambda$ for all q . In our renormalization scheme I also have $\mathcal{M}_{2,s}^{(n)}(0) = \mathcal{K}_{2,s}^{(n)}(0) = 0$ for $n \geq 2$. Since $\mathcal{K}_{2,s}$ has no term linear in q , it follows from Eq. (C1) that

$$\mathcal{M}_{2,s}^{(2)} = \frac{iq}{16\pi E} + \mathcal{O}(q^2). \quad (\text{C2})$$

Substituting this back into Eq. (C1) then yields

$$\mathcal{K}_{2,s}^{(3)} = \mathcal{M}_{2,s}^{(3)} - \frac{q^2}{(16\pi E)^2} + \mathcal{O}(q^3). \quad (\text{C3})$$

¹⁵ This expression holds above threshold. In order that $\mathcal{K}_{2,s}$ be a real, analytic function of q^2 , one must replace iq with $-|q|$ below threshold.

It follows that the imaginary part of $\mathcal{M}_{2,s}^{(3)}$ begins at $\mathcal{O}(q^3)$ and that

$$\left. \frac{d\mathcal{K}_{2,s}^{(3)}}{dq^2} \right|_{\text{thr}} = \left. \frac{d\mathcal{M}_{2,s}^{(3)}}{dq^2} \right|_{\text{thr}} - \frac{1}{(32\pi m)^2}. \quad (\text{C4})$$

The difference between the derivatives of $\mathcal{K}_{2,s}^{(3)}$ and $\mathcal{M}_{2,s}^{(3)}$ arises only from diagrams having two physical cuts. There is in fact only one such diagram—the SS diagram to be discussed shortly. For all other diagrams the threshold derivatives of $\mathcal{K}_{2,s}^{(3)}$ and $\mathcal{M}_{2,s}^{(3)}$ are the same, and so I can calculate the latter.

The diagrams that contribute to $\mathcal{M}_{2,s}^{(3)}$ are those of Fig. 1, for which I use the same names as in the calculation of $C_{2,\text{thr}}^{(3)}(0)$ in Sec. III A. Each two-loop diagram is combined with the same counterterm diagrams as described in Sec. III A.

a. SS diagram, Fig. 1(d)

This diagram factorizes into two single s-channel loops, along with corresponding counterterms. Each of these begins at $\mathcal{O}(q)$ with the imaginary term resulting from the cut, leading to

$$\mathcal{M}_{2,s}^{(3,SS)} = - \left(\frac{iq}{16\pi E} \right)^2 + \mathcal{O}(q^3). \quad (\text{C5})$$

This contribution exactly cancels that appearing in Eq. (C3), so that

$$\mathcal{K}_{2,s}^{(3,SS)} = \mathcal{O}(q^3). \quad (\text{C6})$$

Thus this diagram gives no contribution to $d\mathcal{K}_{2,s}/dq^2$ at threshold.¹⁶

b. TT diagram, Fig. 1(e)

The result again factorizes, but in this case the contribution of each loop is proportional to q^2 because there is no imaginary part (and because the loop plus counterterm vanishes at threshold). Thus the product of the two loops is proportional to q^4 and gives no contribution to desired derivative.

c. SU diagram, Fig. 1(f)

Figure 1(f) combines with the A_{3su} contribution to Fig. 1(a), together with the $A_{2s} + A_{2u}$ contribution to Fig. 1(c), and their vertical reflections. In fact, the contribution proportional to A_{3su} is independent of q^2 , and so can be ignored here.

To evaluate the diagram I follow the method described in Ref. [12]. I use the momentum labels shown in Fig. 1(f). Including the vertical reflection and the contraction with q_3 and q_4 interchanged, I find

$$i\mathcal{M}_{2,\text{bare}}^{(3,SU)} = 2(-i)^3 \int_{p,k} \Delta(p+q_1)\Delta(p+q_4)\Delta(p+k)\Delta(k), \quad (\text{C7})$$

where $\Delta(p) = i/(p^2 - m^2 + i\epsilon)$, and “bare” indicates that the counterterm has not yet been included. Throughout this appendix, and in contradistinction to the main text and the other appendices, I use p, k, \dots to refer to four-momenta, and the shorthand $\int_p = \int d^d p / (2\pi)^d$ for the dimensionally regulated four-momentum integral.

From Eq. (C7) it is clear that the only Lorentz invariant combinations of external momenta that can appear are $q_1^2 = m^2$, $q_4^2 = m^2$ and $(q_1 - q_4)^2 = t$. Dependence on q^2 enters only through $t = -2q^2(1 - \cos\theta_{14})$, and the derivative

¹⁶ One can also understand this result by noting that the iq terms arise from the use of the $i\epsilon$ pole prescription and are absent when using the PV prescription appropriate for $\mathcal{K}_{2,s}$.

with respect to q^2 at threshold thus picks out the term linear in t . Since in this term the s -wave projection averages $\cos\theta_{14}$ to zero, it follows that

$$\left. \frac{d\mathcal{K}_{2,s}^{(3,SU)}}{dq^2} \right|_{\text{thr}} = -2 \left. \frac{d\mathcal{M}_2^{(3,SU)}}{dt} \right|_{\text{thr}}. \quad (\text{C8})$$

This equality also holds for the counterterm diagram Fig. 1(c), since it also depends only on t .

Introducing Feynman parameters x and y for the k and p integrals, respectively, performing the k integral, and combining denominators using Eq. (10.56) of Ref. [12], I reach¹⁷

$$i\mathcal{M}_{2,\text{bare}}^{(3,SU)} = -2 \int_y \int_x \int_w (1-w) w^{1-d/2} \frac{\Gamma(4-d/2)}{(4\pi)^{d/2}} \int_p \frac{1}{D_{SU}^{4-d/2}}, \quad (\text{C9})$$

where the factor in the denominator is

$$D_{SU} = w [m^2 - x(1-x)p^2] + (1-w) [m^2 - p^2 - y(2p \cdot q_1 + q_1^2) - (1-y)(2p \cdot q_4 + q_4^2)], \quad (\text{C10})$$

and the y , x and w integrals range from 0 to 1. Expanding out D_{st} and completing the square by shifting from p to p' (whose explicit form is not needed) leads to

$$D_{SU} = -\gamma p'^2 + m^2 + \Delta_{st}, \quad (\text{C11})$$

$$\gamma = 1 - w + wx(1-x), \quad (\text{C12})$$

$$\Delta_{SU}(w) = \frac{1-w}{\gamma} \{-m^2 wx(1-x) - t(1-w)y(1-y) - (q_4^2 - m^2)wx(1-x)(1-y)\}. \quad (\text{C13})$$

Here I have set $q_1^2 = m^2$, but shown the q_4^2 dependence for later use in the discussion of $\mathcal{M}_{3,\text{thr}}$. In the rest of this subsection I will set $q_4^2 = m^2$. Note that, although Δ_{su} depends on w , x , y and t , it is convenient to show only its dependence on w explicitly. Performing the p integral leads to the result

$$\mathcal{M}_{2,\text{bare}}^{(3,SU)} = -2 \frac{\Gamma(4-d)}{(4\pi)^d} \int_y \int_x \int_w \frac{(1-w)w^{1-d/2}}{\gamma^{d/2}} \frac{1}{(m^2 + \Delta_{SU}(w))^{4-d}}. \quad (\text{C14})$$

The denominator $m^2 + \Delta_{SU}(w)$ does not vanish in the physical region ($t \leq 0$).

The result (C14) has an explicit UV pole from the $\Gamma(4-d)$, and the integral over w near 0 leads to a second pole. Lying underneath the double-pole is a momentum-dependent single pole. This is canceled by the contribution from the counterterm diagram Fig. 1(c), which yields

$$\mathcal{M}_{2,\text{ct}}^{(3,SU)} = 2 \frac{\Gamma(2-d/2)^2}{(4\pi)^d (m^2)^{2-d/2}} F_{SU} \int_0^1 dy \frac{1}{(m^2 + \Delta_{SU}(0))^{2-d/2}}. \quad (\text{C15})$$

The factor of

$$F_{SU} = \frac{1 + 1/(d-3)}{2} = 1 - \frac{d-4}{2} + \dots \quad (\text{C16})$$

arises from the counterterm $A_{2s} + A_{2u}$ [see Eqs. (B4) and (B5)].

Combining Eqs. (C14) and (C15) in a way that allows the double pole to be made explicit gives

$$\begin{aligned} \mathcal{M}_2^{(3,SU)} &= -2 \frac{\Gamma(4-d)}{(4\pi)^d} \int_y \int_x \int_w w^{1-d/2} \left[\frac{(1-w)}{\gamma^{d/2}} \frac{1}{(m^2 + \Delta_{SU}(w))^{4-d}} - \frac{1}{(m^2 + \Delta_{SU}(0))^{4-d}} \right] \\ &\quad - 2 \frac{1}{(4\pi)^d} \int_y \left[\frac{\Gamma(4-d)}{2-d/2} \frac{1}{(m^2 + \Delta_{SU}(0))^{4-d}} - \frac{\Gamma(2-d/2)^2 F_{SU}}{(m^2)^{2-d/2}} \frac{1}{(m^2 + \Delta_{SU}(0))^{2-d/2}} \right]. \end{aligned} \quad (\text{C17})$$

Strictly speaking this is not the full renormalized result for the amplitude: the first integral leads to a momentum-independent single pole that will be cancelled by the A_{3su} counterterm, while the second leads to momentum-independent double and single poles that will similarly be canceled. However, these poles are irrelevant for the momentum dependence of interest here.

¹⁷ For brevity, in the following I set the scale introduced by dimensional regularization, μ , equal to unity. The final answer does not depend on μ .

Evaluating the derivative with respect to t and setting $t = 0$, I find an expression in which one can set $d = 4$:

$$\left. \frac{d}{dt} \mathcal{M}_{2,s}^{(3,SU)} \right|_{\text{thr}} = -2 \frac{1}{(4\pi)^4 m^2} \left\{ \int_y \int_x \int_w \frac{y(1-y)}{w} \left[\frac{(1-w)^3}{\gamma^2 [\gamma - w(1-w)x(1-x)]} - 1 \right] - \frac{1}{6} \right\}. \quad (\text{C18})$$

The expression in curly braces has the numerical value $I^{\text{SUr}} = -0.274156$. Converting to the desired derivative using Eq. (C8) leads to the final result:

$$\mathcal{K}'_{2,s}{}^{(3,SU)} \equiv m^2 \left. \frac{d\mathcal{K}_{2,s}^{(3,SU)}}{dq^2} \right|_{\text{thr}} = \frac{I^{\text{SUr}}}{2^6 \pi^4}. \quad (\text{C19})$$

I have checked this result in two ways. The first is to calculate $\mathcal{M}_{2,s}^{(3,SU)}$ using a finite-volume correlation function in which the external momenta are nonvanishing. The second involves relating the SU result to that from the ST diagram by crossing and then calculating the desired derivative for the ST diagram using an unsubtracted dispersion relation. This in turn requires the imaginary part of the amplitude from the ST diagram, which can be obtained from the results in the following subsection.

d. ST diagram, Fig. 1(g)

The calculation proceeds as for the SU diagram, except for the following changes. First, the number of Wick contractions differs, leading to a reduction by an overall factor by two. Second, the counterterm contribution here is proportional to $A_{2t} + A_{2u}$, so F_{SU} is replaced by $F_{ST} = 1$. Finally, the crossing transformation needed to go from the SU to the ST diagram necessitates the substitutions $q_4 \rightarrow q_3$ and $q_1 \rightarrow -q_4$. This implies that $t = (q_1 - q_4)^2$ is replaced by $(q_3 + q_4)^2 = s$, so $\mathcal{M}_{2,s}^{(3,ST)}$ is pure s-wave. Since $s = 4(q^2 + m^2)$ the desired derivative is given by

$$\left. \frac{d\mathcal{K}_{2,s}^{(3,ST)}}{dq^2} \right|_{\text{thr}} = 4 \left. \frac{d\mathcal{M}_{2,s}^{(3,ST)}}{ds} \right|_{\text{thr}}, \quad (\text{C20})$$

where threshold occurs at $s = 4m^2$. Since the ST diagram has a physical cut, $\mathcal{M}_{2,s}^{(3,ST)}$ has an imaginary part, but, as explained above, this begins only at $\mathcal{O}(q^3)$, and does not contribute to the derivative at threshold.

Thus I find that $\mathcal{M}_{2,s}^{(3,ST)}$ is given by Eq. (C17) except that the overall factor of 2 is dropped, $F_{SU} \rightarrow 1$, and $\Delta_{SU}(w)$ is replaced by

$$\Delta_{ST}(w) = \frac{1-w}{\gamma} \left\{ -m^2 w x(1-x) - s(1-w)y(1-y) - (q_3^2 - m^2) w x(1-x)(1-y) \right\}, \quad (\text{C21})$$

Here I have set $q_4^2 = m^2$ but kept the dependence on q_3^2 explicit for use in the calculation of $\mathcal{M}_{3,\text{thr}}$. For the rest of this subsection, however, I set $q_3^2 = m^2$.

The calculation in this case is more challenging than for the SU diagram because individual terms lead to a diverging derivative at threshold that becomes finite only when they are combined. Thus I proceed somewhat differently, expanding about $d = 4$ and keeping only s -dependent part, which is finite and has the form

$$\mathcal{M}_{2,s}^{(3,ST)} \supset \frac{1}{(4\pi)^4} \left\{ \iiint_0^1 dy dx dw \frac{1}{w} \left[\frac{(1-w)}{\gamma^2} \log D_{ST}(w) - \log D_{ST}(0) \right] - \frac{1}{2} \int_0^1 dy [\log D_{ST}(0)]^2 \right\}, \quad (\text{C22})$$

where

$$D_{ST}(w) = 1 + \Delta_{ST}(w)/m^2. \quad (\text{C23})$$

As long as $s < 4m^2$ all terms are real, and the y integrals can be done analytically. Doing the remaining w and x integrals numerically, and then determining the s derivative also numerically, I find

$$\mathcal{K}'_{2,s,\text{thr}}{}^{(3,ST)} = 4m^2 \left. \frac{d\mathcal{M}_{2,s}^{(3,ST)}}{ds} \right|_{\text{thr}} = \frac{I^{\text{STr}}}{(4\pi)^4}, \quad I^{\text{STr}} = 1.14009. \quad (\text{C24})$$

I have checked this result using an unsubtracted dispersion relation for $d\mathcal{M}_{2,s}^{(3,ST)}/ds$.

2. Calculation of $\mathcal{M}_{2,\text{off}}^{(3)}$

The off-shell two-loop two-particle scattering amplitude is needed in the determination of $\mathcal{M}_{3,\text{thr}}$ in Secs. IV B 11, IV B 13 and IV B 14. The calculation of this amplitude is closely related to that of the effective range from the ST and SU diagrams described above.

a. ST diagram

As explained in Sec. IV B 11, what is needed is the amplitude $\mathcal{M}_{2,\text{off}}^{(3,\text{ST})}$, which arises from Fig. 1(g) when q_3 is off shell while the remaining external legs are on shell. The form of the result has already been described in Sec. C 1 d: it is given by Eq. (C17) except that F_{SU} is set to unity, and Δ_{SU} is replaced by

$$\Delta_{\text{ST,off}}(w) = \frac{1-w}{\gamma} \{-m^2 wx(1-x) - s(1-w)y(1-y) - \delta wx(1-x)(1-y)\}. \quad (\text{C25})$$

Here I have parametrized the off-shellness of q_3 by

$$\delta = q_3^2 - m^2. \quad (\text{C26})$$

There is one difference from Sec. C 1 d, which concerns the overall factor. In Eq. (C17) this is 2, while in Sec. C 1 d it is 1. Here it changes to 1/2, because the horizontal reflection (the TS diagram) does not contribute to $\mathcal{M}_{3,\text{thr}}$, as explained in Sec. IV B 10.

The specific quantity of interest is the difference between off- and on-shell amplitudes defined in Eq. (130), which [noting that q in Eq. (130) is called q_3 here] is given by

$$\mathcal{M}_{3,\text{thr}}^{(4,\text{STf})} = 2 \times 9 \times \left. \frac{d\mathcal{M}_{2,\text{off}}^{(3,\text{ST})}}{d\delta} \right|_{s=4m^2, \delta=0}. \quad (\text{C27})$$

The factor of 2 arises from the horizontal reflection, and the 9 results from symmetrization. Noting that $\Delta_{\text{ST,off}}(0)$ is independent of δ , I find

$$\left. \frac{d\mathcal{M}_{2,\text{off}}^{(3,\text{ST})}}{d\delta} \right|_{s=4m^2, \delta=0} = \frac{1}{2} \frac{1}{(4\pi)^4} \int_y \int_x \int_w \frac{(1-w)}{\gamma^2 w} \left\{ \frac{1}{m^2 + \Delta_{\text{ST,off}}(w)} \frac{d\Delta_{\text{ST,off}}(w)}{d\delta} \right\} \Big|_{s=4m^2, \delta=0}, \quad (\text{C28})$$

$$\equiv \frac{1}{2} \frac{1}{(4\pi)^4 m^2} I^{\text{STM}}, \quad I^{\text{STM}} = -0.214978. \quad (\text{C29})$$

In the first line I have set $d = 4$ since the result is finite, and in the second performed the numerical evaluation of the integral. Substituting this result in Eq. (C27) leads to the result quoted in the main text, Eq. (131).

b. SU diagram

Here the calculation turns out to be identical to that of Sec. C 1 c, aside from overall factors. This is because the off-shellness enters only through t , so $\Delta_{\text{SU}}(w)$ retains the same form as in the on shell case. The overall factor is reduced by two because here SU and US diagrams must be considered separately. Thus I find

$$\mathcal{M}_{2,\text{off}}^{(3,\text{SU})}(t) = \frac{1}{2} \mathcal{M}_{2,s}^{(3,\text{SU})}(t). \quad (\text{C30})$$

The contribution to $\mathcal{M}_{3,\text{thr}}$ is

$$\mathcal{M}_{3,\text{thr}}^{(4,\text{SUf})} = 18 \left. \frac{d\mathcal{M}_{2,\text{off}}^{(3,\text{SU})}}{d\delta} \right|_{t=0, \delta=0} \quad (\text{C31})$$

$$= \frac{9}{2} \left. \frac{d\mathcal{M}_{2,s}^{(3,\text{SU})}}{dt} \right|_{t=0}. \quad (\text{C32})$$

where in the second step I have used

$$t = \frac{1}{2}\delta - \frac{1}{2}(s - 4m^2), \quad (\text{C33})$$

as well as Eq. (C30). The required derivative is given in Eq. (C18),

$$\left. \frac{d\mathcal{M}_{2,s}^{(3,\text{SU})}}{dt} \right|_{t=0} = -\frac{2I^{\text{SUr}}}{(4\pi)^4 m^2}. \quad (\text{C34})$$

Inserting this into Eq. (C32) gives the result quoted in the main text, Eq. (136).

c. US diagram

The contribution of the US diagram to $\mathcal{M}_{3,\text{thr}}$ differs from that for the SU fish diagram because, when Fig. 1(g) is vertically reflected, q_4 and q_3 are interchanged. Thus Δ_{SU} is replaced by

$$\Delta_{\text{US,off}}(w) = \frac{1-w}{\gamma} \left\{ -m^2 w x(1-x) - t(1-w)y(1-y) - \delta w x(1-x)(1-y) \right\}, \quad (\text{C35})$$

with t still given by Eq. (C33). The contribution to $\mathcal{M}_{3,\text{thr}}$ is thus

$$\mathcal{M}_{3,\text{thr}}^{(4,\text{USf})} = 18 \left. \frac{d\mathcal{M}_{2,\text{off}}^{(3,\text{US})}}{d\delta} \right|_{t=0,\delta=0} \quad (\text{C36})$$

$$= \frac{9}{2} \left. \frac{d\mathcal{M}_{2,s}^{(3,\text{SU})}}{dt} \right|_{t=0} - \frac{9}{(4\pi)^4 m^2} \left\{ \int_y \int_x \int_w \frac{(1-w^2)}{\gamma^2} \frac{2x(1-x)(1-y)}{\gamma - w(1-w)x(1-x)} \right\}, \quad (\text{C37})$$

$$\equiv \frac{9}{(4\pi)^4 m^2} I^{\text{USM}}, \quad I^{\text{USM}} = 0.096623. \quad (\text{C38})$$

To obtain the final result I have used Eq. (C34) and the fact that the triple integral in Eq. (C37) evaluates to -0.177533 . Combining this result with Eq. (138) leads to the result quoted in the main text, Eq. (139).

- [1] M. Luscher, *Commun.Math.Phys.* **105**, 153 (1986).
- [2] M. Luscher, *Nucl.Phys.* **B354**, 531 (1991).
- [3] M. T. Hansen and S. R. Sharpe, *Phys. Rev.* **D90**, 116003 (2014), arXiv:1408.5933 [hep-lat].
- [4] M. T. Hansen and S. R. Sharpe, (2015), arXiv:1504.04248 [hep-lat].
- [5] R. A. Briceño, M. T. Hansen, and S. R. Sharpe, *Phys. Rev.* **D95**, 074510 (2017), arXiv:1701.07465 [hep-lat].
- [6] H. W. Hammer, J. Y. Pang, and A. Rusetsky, (2017), arXiv:1706.07700 [hep-lat].
- [7] H. W. Hammer, J. Y. Pang, and A. Rusetsky, (2017), arXiv:1707.02176 [hep-lat].
- [8] M. T. Hansen and S. R. Sharpe, *Phys. Rev.* **D93**, 096006 (2016), [Erratum: *Phys. Rev.*D96,no.3,039901(2017)], arXiv:1602.00324 [hep-lat].
- [9] M. T. Hansen and S. R. Sharpe, *Phys. Rev.* **D93**, 014506 (2016), arXiv:1509.07929 [hep-lat].
- [10] C. Kim, C. Sachrajda, and S. R. Sharpe, *Nucl.Phys.* **B727**, 218 (2005), arXiv:hep-lat/0507006.
- [11] S. R. Beane, W. Detmold, and M. J. Savage, *Phys.Rev.* **D76**, 074507 (2007), arXiv:0707.1670 [hep-lat].
- [12] M. E. Peskin and D. V. Schroeder, *An Introduction to quantum field theory* (1995).